

---

# Improving Generative Methods for Causal Evaluation via Simulation-Based Inference

---

**Pracheta Amaranath**

Manning College of Information and Computer Sciences,  
University of Massachusetts Amherst,  
Amherst, MA 01002  
pboddavarama@umass.edu

**Vinitra Muralikrishnan**

Manning College of Information and Computer Sciences,  
University of Massachusetts Amherst,  
Amherst, MA 01002  
vmuralikrish@umass.edu

**Amit Sharma**

Microsoft Research  
Bengaluru, India  
amshar@microsoft.com

**David D. Jensen**

Manning College of Information and Computer Sciences,  
University of Massachusetts Amherst,  
Amherst, MA 01002  
jensen@cs.umass.edu

## Abstract

Generating synthetic datasets that accurately reflect real-world observational data is critical for evaluating causal estimators, but remains a challenging task. Existing generative methods offer a solution by producing synthetic datasets anchored in the observed data (*source data*) while allowing variation in key parameters such as the treatment effect and amount of confounding bias. However, existing methods typically require users to provide point estimates of such parameters (rather than distributions) and fixed estimates (rather than estimates that can be improved with reference to the source data). This denies users the ability to express uncertainty over parameter values and removes the potential for posterior inference, potentially leading to unreliable estimator comparisons. We introduce *simulation-based inference for causal evaluation (SBICE)*, a framework that models generative parameters as uncertain and infers their posterior distribution given a source dataset. Leveraging techniques in simulation-based inference, SBICE identifies parameter configurations that produce synthetic datasets closely aligned with the source data distribution. Empirical results demonstrate that SBICE improves the reliability of estimator evaluations by generating more realistic datasets, which supports a robust and data-consistent approach to causal benchmarking under uncertainty.

## 1 Introduction

A central challenge in causal inference is evaluating the accuracy of causal estimators. This is a difficult task due to the fundamental problem of causal inference [Holland, 1986] — we only observe the outcome under the assigned treatment group for each unit. In contrast to associational machine learning, where ground truth labels enable cross-validation with held-out data, causal inference

almost always lacks direct access to counterfactual outcomes or ground truth estimates, making such cross-validation techniques infeasible.

These challenges are exacerbated when we wish to evaluate causal estimators for a specific, real-world dataset (referred to henceforth as the *source* dataset). Existing approaches use synthetic and semi-synthetic datasets as benchmarks [Dorie et al., 2019], but they are not designed to reflect the specific assumptions or characteristics of a given source dataset. Recent approaches use generative neural networks [Parikh et al., 2022, Neal et al., 2020, de Vassimon Manela et al., 2024] to approximate the distribution of the source data and potentially generate counterfactual outcomes. We refer to such methods as *generative methods* and focus on their use for generating synthetic datasets for causal evaluation.

The goal of generative methods is to produce a distribution of datasets that correspond to: (1) what can be inferred from the source data; and (2) domain-specific prior knowledge (e.g., plausible treatment effect size or the presence of unobserved confounding). Each generative method encodes this information in different ways, by incorporating user-defined parameters into the generation process. These parameters directly or indirectly influence confounding bias, selection bias, treatment propensity (overlap), unobserved confounding, and treatment heterogeneity in the generated datasets. We refer to these parameters as *data generating process (DGP) parameters* henceforth, as they pertain to parameters that are specified as part of the data generating process.<sup>1</sup>

The specification of DGP parameters is central to evaluating the sensitivity of causal estimators and using a plausible range of values remains critical for robust evaluation. Generation of realistic datasets is the first step in this evaluation, and it is critical for downstream tasks such as estimator ranking or sensitivity analysis. In this paper, we focus on that first step — generating datasets that correspond to prior knowledge and what can be inferred from the source data. Existing generative approaches allow users to fix DGP parameters to point estimates informed by domain knowledge, from which synthetic datasets can be generated. However, these methods vary substantially in how they encode such assumptions, and how changes in DGP parameters propagate through the generation process. As we demonstrate in Section 2, incompatible choices of DGP parameters can distort the evaluation of causal estimators by inducing synthetic datasets that poorly represent the underlying source data. Moreover, most current methods do not explicitly correct for mismatches between the source data distribution and the data generated under a given DGP parameter configuration, increasing the risk of drawing misleading conclusions about estimator performance.

To address this issue, we advocate for generative methods that represent DGP parameters not as fixed values but as distributions that reflect user uncertainty. This perspective enables a more expressive form of sensitivity analysis, where identifiability of causal effects is treated as a continuum: users can encode varying degrees of uncertainty over different parts of the generative model, and some joint configurations of DGP parameters may become more or less probable given the source data.

We propose a principled approach that anchors the choice of DGP parameters in the observed characteristics of the source dataset. Instead of relying on arbitrary or uniformly sampled parameter settings, our method uses simulation-based inference to estimate a posterior distribution over DGP parameters that are consistent with the source data. This posterior captures both the uncertainty in the assumptions and their compatibility with the observed distribution, allowing the method to filter out implausible parameter configurations. By generating datasets from this posterior rather than from a potentially

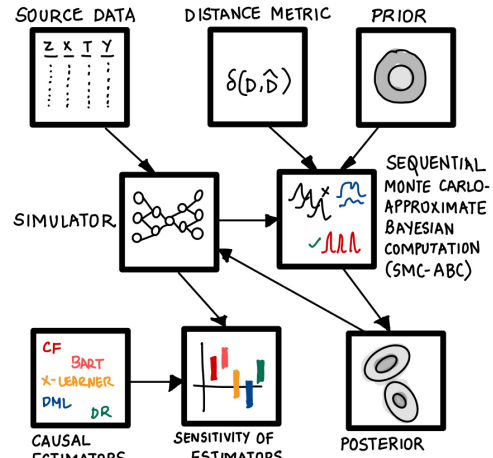


Figure 1: Simulation-based inference for causal evaluation (SBICE)

<sup>1</sup>To be precise, these parameters are the DGP *model* parameters, as they pertain to the parameters that define the model that produces the data as opposed to the actual data generating process which may not conform to simplistic mathematical expressions

uninformative prior, our approach provides more reliable sensitivity analyses and produces estimates of causal estimators closer to that of the source dataset.

We formalize this approach in *simulation-based inference for causal evaluation (SBICE)*, detailed in Section 3. SBICE works by encoding the user’s initial assumptions as a prior and using techniques in simulation-based inference [Cranmer et al., 2020] to infer a posterior over DGP parameters. Generative methods serve as a simulator, enabling likelihood-free inference. This process is illustrated in Figure 1. Importantly, SBICE acts as a wrapper around existing generative methods, enhancing their utility by grounding the generative process in data-informed posterior distributions over DGP parameters, rather than relying on fixed or arbitrary configurations. Admittedly, the improvements of SBICE rely heavily on the ability of the simulator to generate datasets that are close to the source, in the absence of which we see equivalent performance for the posterior and the prior.

This approach offers several key advantages: (1) The generated data distribution more closely aligns to the source data distribution even in the absence of strong prior knowledge about true DGP parameter values; (2) By sampling according to the posterior, our method avoids the naive assumption that all parameter values are equally plausible. In scenarios where the source dataset offers little information about DGP parameters, our approach naturally falls back to a uniform prior, recovering standard sensitivity analysis practices; (3) The posterior distribution supports both marginal and joint sensitivity analyses over DGP parameters; and (4) It facilitates the integration of datasets from multiple generative methods.

Our primary contributions are:

1. **Empirical evaluation of generative methods for sensitivity analysis of causal estimators:** We present a systematic evaluation of existing generative methods for sensitivity analysis of causal estimators. Our study reveals that generative methods often yield inconsistent synthetic datasets, both with respect to each other and to the source dataset. This inconsistency can lead to divergent or misleading assessments of estimator performance.
2. **Improved estimator evaluation through posterior-weighted simulations (SBICE):** We introduce SBICE, a novel simulation-based inference framework that addresses the inconsistency of generated datasets problem by learning a posterior distribution over DGP parameters values consistent with the source data. This approach enables principled filtering of implausible parameter settings and facilitates downstream tasks such as estimator sensitivity analysis and robustness assessment across DGP parameter variations.

**Prior Work** Existing approaches that evaluate causal estimators using synthetic and semi-synthetic datasets [Gentzel et al., 2021, Shimoni et al., 2018, Dorie et al., 2019], or employing surrogate metrics for model selection [Mahajan et al., 2024] are applicable for assessing estimator performance for a broad spectrum of conditions instead of the assumptions or characteristics of a given source dataset. Recent advances in synthetic data generation has allowed researchers to focus on the problem of evaluating causal estimators for a source dataset. These methods generate data that closely approximates the source data distribution and can also generate counterfactual outcomes. Traditionally, this involved fitting parametric or semi-parametric models to the source dataset while attempting to preserve its causal relationships [Schuler et al., 2017]. The advent of flexible, non-parametric generative models, such as generative adversarial networks (GANs) [Athey et al., 2024], variational autoencoders (VAEs) [Parikh et al., 2022], sigmoidal flow networks [Neal et al., 2020] and autoregressive neural spinal flows (Frugal Flows) [de Vassimon Manela et al., 2024], has led to new techniques for generating data with more fidelity to the original causal structure.

Earlier methods have used generative neural networks to approximate counterfactual outcome distributions [Yoon et al., 2018, Shi et al., 2019]. Their goal was to directly estimate causal effects by generating the potential outcomes for each unit. In contrast, recent generative frameworks, including our approach, use these models primarily to evaluate causal estimators, by incorporating DGP parameters that can model prior knowledge. Note that if a generative model is used to simulate the counterfactual distribution, then any estimator that uses the same architecture may recover the counterfactual distribution exactly and minimize estimation bias. Since our focus is on evaluation, varying and treating DGP parameters as uncertain enables systematic assessment of estimator performance under a range of plausible scenarios.

A complementary perspective comes from the literature on Bayesian Causal Inference [Li et al., 2023, Linero and Antonelli, 2023, Hahn et al., 2020, Oganisian and Roy, 2021, McCandless et al., 2007], which models the data-generating process through random variables for the covariate distribution, the assignment mechanism, and potential outcome distribution. Analysts can impose priors on these variables and infer posterior distributions, propagating uncertainty into causal effect estimates. However, modeling choices, such as independence assumptions on the random variables and parametric vs. non-parametric forms need to be explicitly specified by the analyst, and standard Bayesian non-parametrics may be insufficient for high-dimensional data. By contrast, generative neural networks serve as flexible non-parametric representations of the data-generating process, reducing the need for such explicit assumptions.

Relatedly, the source distribution estimation literature [Vetter et al., 2024] considers multiple source distributions compatible with observed data, selecting the maximum-entropy solution. Our objective differs: rather than a single distribution, we aim to extract the full set of plausible generative processes to test causal estimators across diverse yet source-consistent scenarios. This motivates a simulation-based inference framework capable of integrating multiple generative models to yield datasets that are both varied and aligned with the observed distribution.

Compared to existing generative frameworks like Credence [Parikh et al., 2022] and WGANs [Athey et al., 2024], SBICE offers greater flexibility. It supports both domain-informed simulators and data-driven generative models, making it broadly applicable. Unlike Credence, which constrains simulation through training-time hyperparameters, SBICE lets users specify priors over DGP parameters and infers posterior distributions that reflect data fit. Our method also contrasts with generative models like WGANs [Athey et al., 2024], which learn the source data distribution but do not allow controlled variation of DGP parameters for sensitivity analysis over causal parameters. Overall, our work bridges the gap between purely data-driven generative methods and domain-informed simulation approaches.

## 2 Generative methods for evaluating causal estimators

In this section, we investigate existing generative methods to evaluate causal estimators. Generative methods are used to assess the robustness of estimators under various assumptions, by generating synthetic datasets parameterized by the user-specified DGP parameters. We find that current methods often produce datasets that are inconsistent—both with one another and with the observed source dataset—even when configured with identical parameter settings. These inconsistencies can result in diverging or misleading assessments of estimator performance. Our analysis addresses two central questions: (1) How well do generative methods faithfully encode prior knowledge? and (2) How accurately do they infer the probability distribution over possible datasets that align with source data and prior knowledge?

We focus on the average treatment effect (ATE) denoted by  $\tau = \mathbb{E}[Y(1) - Y(0)]$ , where  $Y(t)$  is the outcome under treatment  $t \in [0, 1]$ . We operate under both regimes: identifiable causal effect (when the standard assumptions of unconfoundedness, consistency and positivity are satisfied) and unidentifiable effects (when those assumptions are violated), specifically when there may be omitted variables.

We use four different generative methods: (1) Credence; (2) a modified version of Credence with a different factorization of the joint distribution (called mod-Credence); (3) Realcause; and (4) FrugalFlows. We provide a detailed description of each method in Appendix C. Although each generative method encodes causal assumptions differently via distinct sets of DGP parameters, all require users to specify exact values for DGP parameters, of which some may be inconsistent with the source data, leading to differences in estimator performance. We theoretically ground out this phenomenon in Proposition 2.1.

**Proposition 2.1. Incompatibility of fixed DGP parameters under generative modeling of the source data:** Let  $P(D)$  denote the true distribution of the source data  $D = \{X, T, Y\}$ , for a binary treatment  $T$ , consistent with the DGP parameter:  $\tau^*$ . Let  $\hat{P}(D; \tau)$  represent the distribution of datasets generated using a generative method  $\mathcal{G}$  by enforcing a fixed parameter value  $\tau$ . (i) Under assumptions of identifiability: If  $\hat{P}(D; \tau) \equiv P(D)$ , then there exists a unique value  $\tau = \tau^*$ , and any constraints imposed on the values of  $\tau \neq \tau^*$  results in incompatible generated data distributions:  $\hat{P}(D; \tau) \not\equiv P(D)$ . (ii) Under violations of identifiability (e.g., due to unobserved confounding): There may exist a set of parameter values:  $\mathcal{T} = \{\tau^*, \tau_1, \dots, \tau_k\}$  such that for all  $\tau \in \mathcal{T}$ ,  $\hat{P}(D; \tau) \equiv P(D)$ ,



while any value outside this set, i.e.,  $\tau \notin \mathcal{T}$ , will produce data distributions that are not consistent with  $P(D)$ .

*Proof Sketch.* We provide a proof sketch here and include the full proof in Appendix B. Under the standard assumptions of identifiability, a perfect generative method will match the true distributions  $P(X)$  and  $P(Y | T, X)$ , uniquely determining  $\mathbb{E}[Y | T, X]$  and therefore the ATE as  $\tau^*$ . If a strong constraint  $\tau \neq \tau^*$  is enforced, the resulting conditional distribution  $\hat{P}(Y | T, X)$  must diverge from the true distribution to satisfy the constraint. We demonstrate this by including an example of two different distributions  $P_1(Y | T, X)$  and  $P_2(Y | T, X)$  that have the same value of  $\tau$ . In contrast, when identifiability is violated, even with a perfect generative method, multiple DGP parameters configurations:  $\theta = \{\tau, \rho\}$  (with  $\rho$  being the unobserved confounding parameter) exist that may lead to the same joint distribution  $\hat{P}(D; \theta) \equiv P(D)$ .  $\square$

This proposition highlights that incorrect DGP parameter values may lead to generated datasets that are inconsistent with the source data. This mismatch is especially likely when the generative method does not perfectly represent the true data distribution  $P(D)$ —a common occurrence given the presence of model misspecification or parametric limitations. Under non-identifiability, this mismatch is further compounded by the joint influence of  $\{\tau, \rho\}$  on the generated data, as the way in which unobserved confounding is modeled varies across generative methods. Credence balances constraint satisfaction and fidelity to the source data and models unobserved confounding by sampling from a learned counterfactual distribution, while FrugalFlows models unobserved confounding by introducing correlation between covariates and the causal effect distribution. Realcause does not model unobserved confounding and adjusts ATE, overlap and treatment heterogeneity post hoc. These varying approaches can produce incompatible datasets and complicate tasks like sensitivity analysis and estimator evaluation when the generated data cannot be validated against the source distribution.

**Experiments** We evaluate the differences in generative methods by comparing the bias of 50 datasets from each method, all constrained to the same ATE value  $\tau = c$ . The bias of a causal estimator is defined as the value of the estimated ATE minus the ATE set by the user, which is  $c$ . We use three different settings for  $c$ : (1) the learned ATE (inferred directly from the source data); (2) the true ATE (when ground-truth is known); and (3) an incorrect ATE. Despite fixing  $\tau$ , we observe substantial differences in both the marginal and joint distributions of the resulting datasets. The marginal distribution plots are included in Appendix H. To assess the similarity between generated and source datasets, we trained a classifier and recorded its cross-validated AUC score across the 50 datasets. The mean AUC for each setting and generative method is displayed in Table 1 for the Lalonde (Observational) dataset [LaLonde, 1986], a standard benchmark with a ground-truth ATE from a randomized controlled trial. We found that almost all methods generate datasets that differ from the source data, with the lowest AUC scores for the FrugalFlows method.

We also evaluate variations in causal estimates across different settings of  $\tau$ . Using a fixed set of estimators—X-Learner [Künzel et al., 2019] (Linear and Gradient Boosted Tree (GBT) models), Double Machine Learning [Chernozhukov et al., 2019] (Linear/GBT models), Doubly Robust [Dudík et al., 2014] (labeled Linear DR), BART [Hill, 2011] and TMLE [Van Der Laan and Rubin, 2006]—we compute the bias (estimated ATE minus ground-truth ATE) of each estimator for each setting of  $c$  in Figure 2.

Table 1: Classifier AUCs for Lalonde (Observational) datasets generated by each generative method with a specific setting of the DGP parameters for ATE. We find that none of the generative methods are able to create datasets that are similar to the source distribution, although the AUC for FrugalFlows for all three settings is lower compared to the other generative methods.

	Credence	mod-Credence	Realcause	FrugalFlows
Learned ATE	0.945 $\pm$ 0.004	0.778 $\pm$ 0.003	1.0 $\pm$ 0.0	0.669 $\pm$ 0.013
True ATE	0.959 $\pm$ 0.010	0.831 $\pm$ 0.003	1.0 $\pm$ 0.0	0.656 $\pm$ 0.016
Incorrect ATE	0.970 $\pm$ 0.003	0.999 $\pm$ 0.000	1.0 $\pm$ 0.0	0.673 $\pm$ 0.014

Additionally, we assess how varying the DGP parameter  $\rho$  (which controls unobserved confounding) impacts estimator performance using the FrugalFlows method. Using synthetic data designed in the

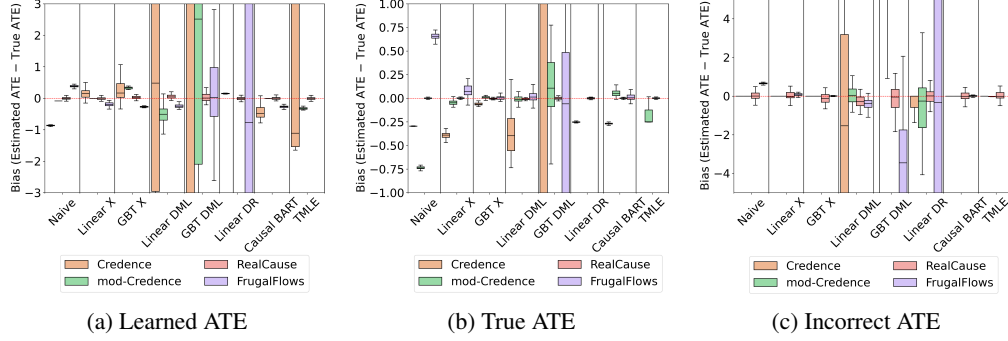


Figure 2: Boxplots of the bias (estimated ATE – true ATE) for a set of causal estimators for all generative methods across three different settings for the Lalonde (Observational) dataset. We note that estimators are inconsistent across different settings and generative methods, emphasizing the impact of setting the right DGP parameter in the generative method.

FrugalFlows [de Vassimon Manela et al., 2024] paper (labeled Frugal DGP2 in our experiments; details included in Appendix F), we systematically vary  $\rho$  during data generation. We find that some estimators, such as the doubly robust estimator (Linear DR), show large variations in performance as  $\rho$  increases (Figure 3). These results highlight the importance of incorporating priors over untestable DGP parameters when supported by the generative model.

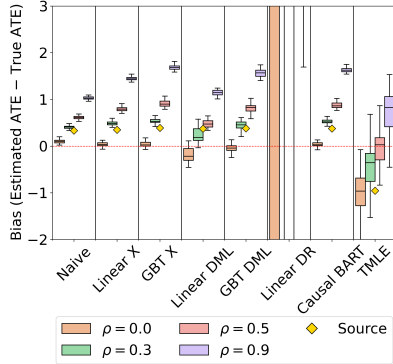


Figure 3: Variation in estimator bias across different values of  $\rho$  (representing unobserved confounding) for Frugal DGP2 generated using FrugalFlows. Estimators such as TMLE and Doubly Robust (Linear) show greater sensitivity to unobserved confounding than others.

**Key Takeaway:** Our analysis shows that while generative methods enable controlled variation in the data-generating process, differences in how methods encode DGP parameters, and how users set them, can lead to substantially different generated data distributions and estimator behaviors. These interactions highlight the importance of generating datasets that closely match the source distribution, motivating our proposed approach.

### 3 Simulation-Based Inference for Causal Evaluation (SBICE)

We improve the reliability of generative methods for benchmarking causal estimators by addressing their reliance on fixed DGP parameters values. Our proposed framework, SBICE, instead models these parameters as uncertain via prior distributions over DGP parameters and estimates a posterior over its values that are consistent with the source data. This posterior captures the set of parameter configurations that plausibly generate data similar to the source dataset and can be used to evaluate estimator performance in a principled, uncertainty-aware manner. If all prior values are equally consistent with the observed data, SBICE reduces to a uniform distribution over the prior.

Let  $\theta$  denote the set of DGP parameters that are implemented by a generative method. In principle, we could compute the posterior  $P(\theta|D)$  using the Bayes theorem:  $P(\theta|D) \propto P(D|\theta)P(\theta)$ . However, the likelihood  $P(D|\theta)$  is typically unknown and intractable for real-world data. Instead, we use a likelihood-free inference method—Approximate Bayesian Computation (ABC) [Nadjahi et al., 2020], specifically Sequential Monte Carlo-ABC (SMC-ABC) [Toni and Stumpf, 2010]. SMC-ABC approximates the posterior by simulating datasets under sampled DGP parameters values and retaining those that closely match the observed data, according to a user-defined distance function and tolerance. This process is illustrated in Figure 1, and an extended algorithm is included in Appendix D.

State-of-the-art SBI algorithms such as neural likelihood estimation (NLE) and neural posterior estimation (NPE) [Cranmer et al., 2020, Lueckmann et al., 2021] train neural networks to approximate the likelihood or posterior directly. While powerful, applying these methods to causal evaluation would require training an additional network on top of a simulation model already learned from limited source data, increasing the risk of misspecification. Unlike physics-based simulators commonly used in traditional SBI, our simulators are data-driven and constrained by the finite sample size of the source dataset. Moreover, NLE and NPE face added challenges in handling mixed discrete–continuous data and in treating an entire dataset as i.i.d. draws from the simulator. For these reasons, we restrict our approach to Sequential Monte Carlo Approximate Bayesian Computation (SMC-ABC), which provides flexibility through a user-defined distance metric. This allows SBICE to both quantify fit to the source data and highlight potential model misspecification: if the simulator cannot generate data that matches the source distribution, SBICE can be deemed inapplicable for that simulator. We now describe each component of SBICE.

**Simulator:** A simulator defines the data-generating process and produces synthetic datasets given DGP parameters values. These may be parametric, with explicit functional forms and DGP parameters encoded as the parameters of the chosen parametric distributions or non-parametric, which uses generative neural networks to model the source data. FrugalFlows and Realcause are examples of non-parametric simulators, as they first learn a flexible generative model from source data and then generate datasets based on the DGP parameters specified by the user.

**Prior:** The prior distribution encodes the user’s belief about plausible values for the DGP parameters. These values can either be informed by domain knowledge or exploratory runs. The priors may be specified as independent or joint distributions, depending on the simulator. The priors may be uniform (non-informative) priors, although informative choices may be used when available.

**Distance and tolerance:** To compare generated and observed datasets, we use a user-defined distance metric  $\delta(\hat{D}, D)$ , which guides parameter proposals and a tolerance  $\epsilon$  that is used as a stopping criteria. Our goal is to minimize the divergence between the joint distributions  $P(D)$  and  $\hat{P}(D)$ . In our experiments, we use the sliced-Wasserstein distance [Nadjahi et al., 2020] due to its efficiency and suitability for high-dimensional data, and choose  $\epsilon$  by empirical tuning.

The posterior distribution,  $P(\theta|D)$  can be used to generate datasets which aid in downstream tasks, such as sensitivity analysis and/or estimator selection. When used for downstream tasks, our approach makes the uncertainty in estimator performance explicit. In cases where multiple estimators have similar posterior performance distributions, SBICE recommends a confidence-aware evaluation rather than a single deterministic ordering. In contrast to standard generative benchmarking, which may spuriously favor estimators due to arbitrary DGP parameters settings, SBICE provides a calibrated and data-consistent framework for estimator comparison.

To summarize, SBICE provides three key improvements over conventional generative benchmarking: (1) It **incorporates uncertainty** over DGP parameters values, reducing sensitivity to arbitrary or misspecified configurations; (2) It leverages posterior inference to focus evaluation on **data distributions that are plausible given the observed data**; and (3) It enables **uncertainty-aware estimator comparison**, highlighting robustness (or lack thereof) in estimator performance.

## 4 Experiments

To evaluate the utility of posterior-weighted datasets for downstream tasks like causal benchmarking and sensitivity analysis, we focus on two key criteria: (1) the distributional alignment between the posterior-weighted and source datasets; and (2) the extent to which the posterior and source datasets exhibit similar performance across all causal estimators. We measure these aspects using two primary metrics, the classifier AUC score and the mean bias squared error (mean BSE) for causal estimators.

Let  $\theta_{\text{post}}$  denote the posterior distribution over the DGP parameters estimated by SBICE, and  $\theta_{\text{prior}}$  the user-defined prior distribution. We define the set of datasets generated from these distributions as  $D_{\text{post}}$  and  $D_{\text{prior}}$  respectively. Let  $D_{\text{source}}$  represent the source dataset, which may be a single dataset (as in real-world settings) or a set of synthetic datasets drawn from the same data-generating process.

**Classifier AUC** This metric assesses the distributional closeness between the posterior-weighted datasets and the source data. If the datasets generated using the posterior are consistent with

the source distribution, a classifier trained to distinguish them should exhibit low discriminatory power. Formally, we train a binary classifier (using random forests)  $R$  to distinguish between the posterior and source datasets, and compute its score  $\text{AUC}_{\text{post}} = \text{AUC}(R_{\text{post}}(\mathcal{D}_{\text{post}}, \mathcal{D}_{\text{source}}))$ . Similarly, we compute  $\text{AUC}_{\text{prior}} = \text{AUC}(R_{\text{prior}}(\mathcal{D}_{\text{prior}}, \mathcal{D}_{\text{source}}))$  where  $R_{\text{post}}$  is the classifier trained to distinguish posterior datasets from the source, and  $R_{\text{prior}}$  is the classifier trained to distinguish prior datasets from the source. A lower AUC for the posterior classifier compared to the prior classifier:  $\text{AUC}_{\text{post}} \leq \text{AUC}_{\text{prior}}$  indicates that the posterior is more consistent with the source distribution, validating the informativeness of the inferred posterior. In the ideal case, the  $\text{AUC}_{\text{post}}$  should approach 0.5, reflecting near-indistinguishability between the two distributions.

**Mean bias squared error (Mean BSE)** This metric compares the performance of causal estimators on the posterior, prior and source datasets. With informative posteriors, we expect there to be similar performance between the posterior and the source, when compared to the prior. Let  $\tau_d^{*(i)} \sim \theta_d$  for  $d \in \{\text{post}, \text{prior}\}$  represent the values of the ATE parameter that is used to generate the posterior and prior dataset  $i$ , for  $i \in [1..N]$ . For each of these datasets,  $\tau_d^{*(i)}$  is the true ATE. For the source dataset, the ground-truth ATE is given by  $\tau^*$ .

We define the mean BSE for the posterior-source datasets and a specific causal estimator  $\mathcal{M}$  as

$$\text{Mean BSE}_{\mathcal{M};\text{post}} = \frac{1}{N} \sum_{i=1}^N \left[ \left( \tau_{\mathcal{M};\text{post}}^{(i)} - \tau_{\text{post}}^{*(i)} \right) - (\tau_{\mathcal{M};\text{source}} - \tau^*) \right]^2$$

Similarly, the mean BSE for the prior-source datasets for the same causal estimator  $\mathcal{M}$  is

$$\text{Mean BSE}_{\mathcal{M};\text{prior}} = \frac{1}{N} \sum_{i=1}^N \left[ \left( \tau_{\mathcal{M};\text{prior}}^{(i)} - \tau_{\text{prior}}^{*(i)} \right) - (\tau_{\mathcal{M};\text{source}} - \tau^*) \right]^2$$

Note that for synthetic datasets for which  $\mathcal{D}_{\text{source}}$  is a set of datasets, we use  $\tau_{\mathcal{M};\text{source}}^{(i)}$  instead. A lower BSE for the posterior:  $\text{Mean BSE}_{\mathcal{M};\text{post}} \leq \text{Mean BSE}_{\mathcal{M};\text{prior}}$  across all estimators indicates that the posterior-weighted datasets exhibit similar performance to that of the source data.

We evaluate SBICE across a suite of synthetic datasets and multiple classes of simulators—both parametric and non-parametric. Our empirical study is designed to answer the following questions: (1) How can SBICE improve upon existing generative methods for benchmarking causal estimators for a given source dataset? (2) Under what conditions does the estimated posterior distribution over DGP parameters provide meaningful insights for benchmarking causal estimators?

**Datasets** We evaluate SBICE using synthetic and real-world datasets. These datasets are categorized into three types, referred to as LinearParam, Frugal and Real DGPs. LinearParam datasets use linear, parametric data-generating functions with a single observed covariate  $X$ , an unobserved covariate  $Z$ , binary treatment  $T$  and outcome  $Y$ . They are mainly used to study the effects of simulator misspecification on SBICE. Frugal DGP datasets are based on the synthetic datasets designed using the frugal parameterization [Evans and Didelez, 2024] method [see de Vassimon Manela et al., 2024, Appendix D]. These datasets introduce more complexity, with 4-10 covariates, non-linear functions and model unobserved confounding. Real DGPs are commonly benchmarks in the causal inference literature, limited by sample size and often lacking a ground-truth ATE. We focus on real datasets with an experimental arm, that gives us a ground-truth ATE estimate.

**Simulators** Our experiments use three simulator types: LinearParam simulators (based on parametric, linear models), FrugalParam simulators (based on frugal parameterization), and FrugalFlows (a non-parametric generative method). The specific DGP parameters implemented for each simulator varies, as detailed in the experiment results. An extensive outline of the results for each dataset and simulator type is provided in Appendices E, F, and G, with key takeaways highlighted here.

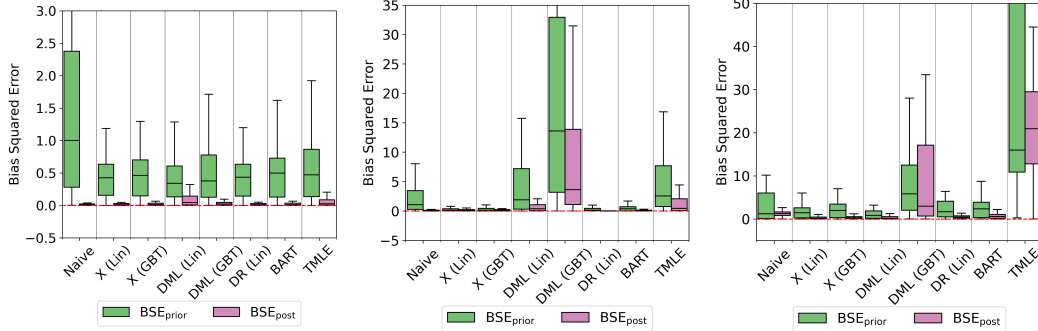
## 4.1 Results

**SBICE produces informative posteriors when the simulator is sufficiently flexible to approximate the joint distribution of the source data.** When the generated datasets closely reflect the

true DGP parameters and the simulator is well-specified, the posterior datasets align with the source data, as shown by the AUC scores in Table 2. We also note that the  $\text{Mean BSE}_{\text{post}} < \text{Mean BSE}_{\text{prior}}$  for all causal estimators. To assess the robustness of SBICE, we systematically introduced model misspecification—such as noise, non-linear functional forms, and changes in parameter identifiability or prior informativeness. We found that, as long as the misspecified simulator could still generate datasets resembling the source, the posterior estimates remained informative and outperformed fixed DGP parameter baselines.

Table 2: Mean BSE scores and classifier AUCs for three synthetic datasets using different types of DGPs and simulators. For all three cases, we conclude that the posterior datasets resemble the source data. This is noted by the a lower  $\text{AUC}_{\text{post}}$  when compared to  $\text{AUC}_{\text{prior}}$ , as well as the lower mean BSE for the posterior datasets.

DGP Simulator	LinearParam DGP1 LinearParam Sim1 $\theta = \{\beta, \tau, \rho\}$		Frugal DGP4 FrugalParam Sim4(u) $\theta = \{\tau, \rho\}$		Frugal DGP4 FrugalFlows Sim4(u) $\theta = \{\tau, \rho\}$	
DGP Param(s)	Prior	Posterior	Prior	Posterior	Prior	Posterior
<b>Mean BSE</b>						
X (Lin)	0.574	0.015	0.277	0.196	1.970	0.315
X (GBT)	0.586	0.019	0.304	0.219	2.187	0.414
DML (Lin)	0.550	0.082	5.144	0.711	1.225	0.438
DML (GBT)	0.564	0.028	34.767	10.531	16.568	12.743
DR (Lin)	8e5	0.016	0.374	0.040	1e6	0.628
BART	0.590	0.018	0.585	0.103	2.447	0.708
TMLE	0.624	0.064	4.809	2.554	48.568	21.787
<b>AUC</b>	<b>0.77 <math>\pm</math> 0.13</b>	<b>0.50 <math>\pm</math> 0.01</b>	<b>0.97 <math>\pm</math> 0.08</b>	<b>0.53 <math>\pm</math> 0.03</b>	<b>0.97 <math>\pm</math> 0.08</b>	<b>0.62 <math>\pm</math> 0.01</b>



(a) Dataset: LinearParam DGP1, Simulator: LinearParam Sim1 (b) Dataset: Frugal DGP4, Simulator: FrugalParam Sim4(u) (c) Dataset: Frugal DGP4, Simulator: FrugalFlows Sim4(u)

Figure 4: We plot the BSE for a set of causal estimators for the datasets in Table 2. Lower BSE values for the posterior indicate similarity to the source dataset.

**Prior and posterior are equivalent when some causal estimators are insensitive to DGP parameters variations** SBICE is most effective when the source data provides a clear signal about the DGP parameter values and the simulator can accurately approximate the source distribution. However, when the DGP parameters are poorly identified or the priors are too narrow or misaligned with the true values, the posterior and prior can yield similar estimator performance, highlighting the need for flexible simulators and appropriately broad priors.

Table 3 presents two illustrative cases. In Frugal DGP3, the posterior closely mirrors the prior because all prior values generate datasets that resemble the source. Using a narrow prior centered on the true treatment effect  $\tau^*$  leads to nearly identical classifier AUCs and mean BSEs for both posterior and prior datasets, indicating insufficient data signal to update the prior. In contrast, Frugal DGP5 displays a lower  $\text{AUC}_{\text{post}}$ , yet estimator performance remains stable, as many causal estimators are

largely insensitive to the specific DGP parameters being varied (except for the Double ML estimators). These cases demonstrate that SBICE can identify when the source data constrains the DGP parameter values and when parameter variations have little impact on estimator performance, reducing the risk of overconfident inferences.

Table 3: BSE and classifier AUCs for two synthetic datasets: Frugal DGP3 and Frugal DGP5 and a real-world dataset: Lalonde (Obs). For the synthetic data,  $\text{BSE}_{\mathcal{M};\text{post}} = \text{BSE}_{\mathcal{M};\text{prior}}$  for nearly all the causal estimators  $\mathcal{M}$  with the exception of the DML estimator (highlighted below). Note the high AUC scores for the Lalonde (Obs) dataset signifying that the simulator was unable to approximate the distribution of the source data.

Dataset Simulator DGP Param(s)	Frugal DGP3 FrugalFlows Sim3 $\theta = \{\tau\}$		Frugal DGP5 FrugalFlows Sim5 $\theta = \{\tau\}$		Lalonde (Obs) FrugalFlows Real2 $\theta = \{\tau\}$	
	Prior	Posterior	Prior	Posterior	Prior	Posterior
<b>Mean BSE</b>						
X (Lin)	0.001	0.001	0.064	0.064	0.805	0.805
X (GBT)	0.002	0.002	0.040	0.040	0.843	0.845
DML (Lin)	0.002	0.002	<b>0.319</b>	<b>0.178</b>	2.622	2.310
DML (GBT)	0.003	0.003	<b>2.172</b>	<b>1.876</b>	248.36	254.512
DR (Lin)	0.001	0.001	1249.36	1249.37	$\approx 2e7$	$\approx 2e7$
BART	0.001	0.001	0.052	0.052	1.158	1.158
TMLE	0.011	0.011	0.790	0.789	2.198	2.445
<b>AUC</b>	$0.54 \pm 0.01$	$0.53 \pm 0.01$	$0.97 \pm 0.05$	$0.65 \pm 0.00$	$0.773 \pm 0.003$	$0.758 \pm 0.005$

**Posterior and prior equivalence in small samples and/or non-informative settings** We evaluate SBICE on three real-world datasets: Lalonde (Exp), Lalonde (Obs) and Project STAR using FrugalFlows as the simulator. For these experiments, we estimate the posterior over the treatment effect parameter  $\tau$ , assuming no unobserved confounding ( $\rho = 0.0$ ). Table 4 presents the classifier AUC results, with additional BSE values provided in Appendix G. The high AUC scores indicate a key limitation of SBICE—when the simulator lacks sufficient flexibility or the source dataset is non-informative, the inferred posterior can closely resemble the prior, providing little additional insight.

Table 4: Classifier AUCs for three real-world datasets using FrugalFlows as the simulator.

Dataset	Prior-Source AUC	Posterior-Source AUC
Real DGP1 (Lalonde (Exp))	$0.967 \pm 0.010$	$0.956 \pm 0.014$
Real DGP2 (Lalonde (Obs))	$0.773 \pm 0.003$	$0.758 \pm 0.005$
Real DGP3 (Project STAR)	$0.939 \pm 0.003$	$0.929 \pm 0.001$

## 5 Conclusion

We addressed the problem of generating datasets that resemble a real-world dataset focusing on approaches that use non-parametric neural network-based simulators. We observed that existing methods often misrepresent the source data distribution under user-specified DGP parameters and lack explicit mechanisms to assess this mismatch. To address this, we introduced SBICE, a principled framework that incorporates uncertainty over DGP parameters through prior distributions and generates synthetic datasets that are better aligned with the source distribution. This approach naturally filters out implausible parameter settings, reducing the risk of biased or misleading conclusions for downstream tasks. In the future, we plan to extend SBICE to simultaneously infer both the generative model and its parameters, enabling principled model selection across generative methods. This broader approach has the potential to produce richer, more diverse benchmark datasets for evaluating causal estimators.

## Acknowledgments and Disclosure of Funding

We thank Purva Pruthi, Andrew Zane and Sankaran Vaidyanathan for helpful discussions on this manuscript.

## References

- Paul W. Holland. Statistics and causal inference. *Journal of the American Statistical Association*, 81 (396):945–960, 1986.
- Vincent Dorie, Jennifer Hill, Uri Shalit, Marc Scott, and Dan Cervone. Automated versus do-it-yourself methods for causal inference: Lessons learned from a data analysis competition. 2019.
- Harsh Parikh, Carlos Varjao, Louise Xu, and Eric Tchetgen Tchetgen. Validating causal inference methods. In *International conference on machine learning*, pages 17346–17358. PMLR, 2022.
- Brady Neal, Chin-Wei Huang, and Sunand Raghupathi. Realcause: Realistic causal inference benchmarking. *arXiv preprint arXiv:2011.15007*, 2020.
- Daniel de Vassimon Manela, Laura Battaglia, and Robin J Evans. Marginal causal flows for validation and inference. In *The Thirty-eighth Annual Conference on Neural Information Processing Systems*, 2024.
- Kyle Cranmer, Johann Brehmer, and Gilles Louppe. The frontier of simulation-based inference. *Proceedings of the National Academy of Sciences*, 117(48):30055–30062, 2020.
- Amanda M Gentzel, Purva Pruthi, and David Jensen. How and why to use experimental data to evaluate methods for observational causal inference. In *International Conference on Machine Learning*, pages 3660–3671. PMLR, 2021.
- Yishai Shimoni, Chen Yanover, Ehud Karavani, and Yaara Goldschmidt. Benchmarking framework for performance-evaluation of causal inference analysis. *arXiv preprint arXiv:1802.05046*, 2018.
- Divyat Mahajan, Ioannis Mitliagkas, Brady Neal, and Vasilis Syrgkanis. Empirical analysis of model selection for heterogeneous causal effect estimation. In *The Twelfth International Conference on Learning Representations*, 2024.
- Alejandro Schuler, Ken Jung, Robert Tibshirani, Trevor Hastie, and Nigam Shah. Synth-validation: Selecting the best causal inference method for a given dataset. *arXiv preprint arXiv:1711.00083*, 2017.
- Susan Athey, Guido W Imbens, Jonas Metzger, and Evan Munro. Using wasserstein generative adversarial networks for the design of monte carlo simulations. *Journal of Econometrics*, 240(2): 105076, 2024.
- Jinsung Yoon, James Jordon, and Mihaela Van Der Schaar. Ganite: Estimation of individualized treatment effects using generative adversarial nets. In *International conference on learning representations*, 2018.
- Claudia Shi, David Blei, and Victor Veitch. Adapting neural networks for the estimation of treatment effects. *Advances in neural information processing systems*, 32, 2019.
- Fan Li, Peng Ding, and Fabrizia Mealli. Bayesian causal inference: a critical review. *Philosophical Transactions of the Royal Society A*, 381(2247):20220153, 2023.
- Antonio R Linero and Joseph L Antonelli. The how and why of bayesian nonparametric causal inference. *Wiley Interdisciplinary Reviews: Computational Statistics*, 15(1):e1583, 2023.
- P Richard Hahn, Jared S Murray, and Carlos M Carvalho. Bayesian regression tree models for causal inference: Regularization, confounding, and heterogeneous effects (with discussion). *Bayesian Analysis*, 15(3):965–1056, 2020.
- Arman Oganisian and Jason A Roy. A practical introduction to bayesian estimation of causal effects: Parametric and nonparametric approaches. *Statistics in medicine*, 40(2):518–551, 2021.

- Lawrence C. McCandless, Paul Gustafson, and Adrian Levy. Bayesian sensitivity analysis for unmeasured confounding in observational studies. *Statistics in Medicine*, 26(11):2331–2347, 2007. doi: <https://doi.org/10.1002/sim.2711>. URL <https://onlinelibrary.wiley.com/doi/abs/10.1002/sim.2711>.
- Julius Vetter, Guy Moss, Cornelius Schröder, Richard Gao, and Jakob H Macke. Sourcerer: Sample-based maximum entropy source distribution estimation. *Advances in Neural Information Processing Systems*, 37:88772–88806, 2024.
- Robert J LaLonde. Evaluating the econometric evaluations of training programs with experimental data. *The American economic review*, pages 604–620, 1986.
- Sören R Künzel, Jasjeet S Sekhon, Peter J Bickel, and Bin Yu. Metalearners for estimating heterogeneous treatment effects using machine learning. *Proceedings of the national academy of sciences*, 116(10):4156–4165, 2019.
- Victor Chernozhukov, Denis Chetverikov, Mert Demirer, Esther Duflo, Christian Hansen, Whitney Newey, and James Robins. Double machine learning for treatment and causal parameters. *Econometrics Journal*, 21:C1–C68, 2019.
- Miroslav Dudík, Dumitru Erhan, John Langford, and Lihong Li. Doubly robust policy evaluation and optimization. *Statistical Science*, 29(4):485–511, 2014. ISSN 08834237, 21688745.
- Jennifer L Hill. Bayesian nonparametric modeling for causal inference. *Journal of Computational and Graphical Statistics*, 20(1):217–240, 2011.
- Mark J Van Der Laan and Daniel Rubin. Targeted maximum likelihood learning. *The international journal of biostatistics*, 2(1), 2006.
- Kimia Nadjahi, Valentin De Bortoli, Alain Durmus, Roland Badeau, and Umut Şimşekli. Approximate bayesian computation with the sliced-wasserstein distance. In *ICASSP 2020-2020 IEEE International Conference on Acoustics, Speech and Signal Processing (ICASSP)*, pages 5470–5474. IEEE, 2020.
- Tina Toni and Michael PH Stumpf. Simulation-based model selection for dynamical systems in systems and population biology. *Bioinformatics*, 26(1):104–110, 2010.
- Jan-Matthis Lueckmann, Jan Boelts, David Greenberg, Pedro Goncalves, and Jakob Macke. Benchmarking simulation-based inference. In *International conference on artificial intelligence and statistics*, pages 343–351. PMLR, 2021.
- Robin J Evans and Vanessa Didelez. Parameterizing and simulating from causal models. *Journal of the Royal Statistical Society Series B: Statistical Methodology*, 86(3):535–568, 2024.
- Uri Shalit, Fredrik D. Johansson, and David Sontag. Estimating individual treatment effect: generalization bounds and algorithms, 2017. URL <https://arxiv.org/abs/1606.03976>.
- Yannik Schälte, Emmanuel Klinger, Emad Alamousi, and Jan Hasenauer. pyabc: Efficient and robust easy-to-use approximate bayesian computation. *Journal of Open Source Software*, 7(74):4304, 2022. doi: 10.21105/joss.04304. URL <https://doi.org/10.21105/joss.04304>.
- Keith Battocchi, Eleanor Dillon, Maggie Hei, Greg Lewis, Paul Oka, Miruna Oprescu, and Vasilis Syrgkanis. EconML: A Python Package for ML-Based Heterogeneous Treatment Effects Estimation. <https://github.com/py-why/EconML>, 2019. Version 0.x.
- Vincent Dorie, Hugh Chipman, and Robert McCulloch. dbarts: Discrete bayesian additive regression trees sampler, 2025. URL <https://CRAN.R-project.org/package=dbarts>. R package version 0.9-32.
- Paul Zivich, Cameron Davidson-Pilon, Joanna Diong, Darren Reger, and The Gitter Badger. pzivich/zepid: v0.9.1, October 2022. URL <https://doi.org/10.5281/zenodo.7242696>.



## A Broader Impacts

This paper presents work that aims to advance the field of evaluation of causal inference algorithms. There are many potential societal consequences of our work, none of which must be specifically highlighted here.

## B Inconsistency of arbitrary point estimates with source data distributions

In this section, we prove Proposition 2.1 for two different sets of assumptions on the source data: (i) under the standard assumptions of unconfoundedness, positivity and consistency; and (ii) under the assumption that there are hidden confounders in the data.

- (i) We assume that the causal effect estimate is identifiable given the source data. Under this assumption, we show that accurately estimating the covariate distribution  $P(X)$  and the conditional distribution of the outcome  $P(Y|T, X)$  for the source data constrains the value of the ATE  $\tau$ . However, the converse is not true—fixing the value of  $\tau$  does not uniquely determine the distribution of covariates and conditional outcomes.

*Proof.* The average treatment effect (ATE) is defined as:

$$\tau = \mathbb{E}[Y(1) - Y(0)]$$

Using linearity of expectation,

$$= \mathbb{E}[Y(1)] - \mathbb{E}[Y(0)]$$

Applying the law of iterated expectations,

$$= \mathbb{E}_X[\mathbb{E}[Y(1)|X] - \mathbb{E}[Y(0)|X]]$$

By the assumptions of unconfoundedness, consistency and positivity, we have  $\mathbb{E}[Y(t)|X] = \mathbb{E}[Y|T = t, X]$ . Therefore,

$$\begin{aligned} \tau &= \mathbb{E}_X[\mathbb{E}[Y|T = 1, X] - \mathbb{E}[Y|T = 0, X]] \\ &= \sum_x \left[ \left[ \sum_y P(y|t = 1, x) \right] - \left[ \sum_y P(y|t = 0, x) \right] \right] \cdot P(x) \end{aligned}$$

Let  $P(\cdot)$  represent the source data distribution, and  $\hat{P}_{\mathcal{G}}(\cdot)$  the estimated data distribution from a generative method  $\mathcal{G}$ . If  $P(y|t = 1, x) = \hat{P}_{\mathcal{G}}(y|t = 1, x)$  and  $P(x) = \hat{P}_{\mathcal{G}}(x)$ , then the expected value  $\mathbb{E}[Y|T, X]$  is an unbiased estimate for the (true) source data distribution and subsequently,  $\tau$ . Conversely, for a fixed value  $\tau$ , and unconstrained generated distributions  $\hat{P}_{\mathcal{G}}(\cdot) \neq P(\cdot)$ , there exists multiple distributions of  $P(y|t, x)$  which can have the same expected value  $\mathbb{E}[Y|T, X]$ . We show one such example below.

Let a causal model  $C_1$  be described by the following data-generating process

$$X \sim \mathcal{N}(0, 1)$$

$$T \sim f(X)$$

$$Y_1 \sim X + T$$

The second causal model  $C_2$  is given by

$$X \sim \mathcal{N}(0, 1)$$

$$T \sim f(X)$$

$$Y_2 \sim X + T + g(X, T) - E[g(X, T)|X, T]$$

where  $f(X)$  and  $g(X, T)$  are functions of  $X$  and  $T$ . Note that these can be made more general by treating  $X$  as a vector of covariates or being drawn from any arbitrary distribution. We show this example for simplicity of expression.

Let us compute the ATE for both causal models. Using the above equation we have the ATE for  $C_1$ :  $\tau_1$  given by

$$\begin{aligned}\tau_1 &= \mathbb{E}_X[\mathbb{E}[Y|T=1, X] - \mathbb{E}[Y|T=0, X]] \\ &= \mathbb{E}_X[\mathbb{E}[X] + 1] - \mathbb{E}[X] \\ &= \mathbb{E}_X[1] \\ \tau_2 &= \mathbb{E}_X[\mathbb{E}[X + 1 + g(X, 1) - \mathbb{E}[g(X, 1)|X, 1] - \mathbb{E}[X + g(X, 0) - \mathbb{E}[g(X, 0)|X, 0]] \\ &= \mathbb{E}_X[\mathbb{E}_X[X + 1 + \mathbb{E}[g(X, 1)] - \mathbb{E}[g(X, 1)] - \mathbb{E}[X] + \mathbb{E}[g(X, 0)] - \mathbb{E}[g(X, 0)]] \\ &= \mathbb{E}_X[1]\end{aligned}$$

In both cases, we have the same causal effect parameter, but two different conditional distributions  $P(Y|X, T)$ . In practice, the learned conditional data distributions may not differ from each other as drastically as shown in this example, but in cases when there is a conflict between the user-specified parameter value and the possible conditional distributions that satisfy that assignment, we may see the effects of such variation.  $\square$

- (ii) We now look at consider the setting when the causal effect is unidentifiable from the source data. These can occur due to a variety of reasons, but we focus on the presence of unobserved confounding for our analysis. In the presence of unmeasured confounding, constraining the value of the average treatment effect (ATE) may lead to multiple different distributions of  $P(X, Z)$  and  $P(Y|T, X, Z)$  that are consistent with the given ATE value, while inducing the same observational distribution  $P(Y|T, X)$ .

*Proof.* By definition, we have that the ATE  $\tau$  is given by

$$\tau = \mathbb{E}[Y(1) - Y(0)]$$

As before, using linearity of expectation, we have

$$= \mathbb{E}[Y(1)] - \mathbb{E}[Y(0)]$$

Assuming the presence of both observed covariates  $X$  and unobserved confounders  $Z$  and using the law of iterated expectations, we have

$$= \mathbb{E}_{X,Z}[\mathbb{E}[Y(1)|X, Z] - \mathbb{E}[Y(0)|X, Z]]$$

If  $Z$  was observed, and assuming positivity and consistency, using the backdoor criteria, this is equivalent to

$$= \mathbb{E}_{X,Z}[\mathbb{E}[Y|T=1, X, Z] - \mathbb{E}[Y|T=0, X, Z]]$$

Writing out the above expression in terms of probability distributions, we have

$$\begin{aligned} &= \sum_{x,z} P(x, z) \left[ \sum_y y \cdot P(y|t=1, x, z) - \right. \\ &\quad \left. \sum_y y \cdot P(y|t=0, x, z) \right] \end{aligned}$$

Using the law of total probability, we write the distribution of  $P(X, Z) = P(Z|X) \cdot P(X)$

$$\begin{aligned} &= \sum_x P(x) \left[ \sum_z P(z|x) \sum_y y \cdot P(y|t=1, x, z) \right. \\ &\quad \left. - \sum_z P(z|x) \sum_y y \cdot P(y|t=0, x, z) \right] \end{aligned} \tag{1}$$

Much like the earlier example, we can construct two different causal models  $C_3$  and  $C_4$  such that they have the same marginal distribution  $P(Y|T, X)$  but different conditional distributions  $P(Y|T, X, Z)$ . For example, let  $C_3$  be

$$X \sim \mathbb{1}(\mathcal{U} < 0.5)$$

$$T \sim \text{Bern}(2X)$$

$$Z_1 \sim \mathbb{1}(\mathcal{U} < 0.5)$$

$$Y_1 \sim X + T + Z_1 - \mathbb{E}[Z_1|X, T] + \epsilon, \epsilon \sim \mathcal{N}(0, 1)$$

where  $\mathbb{E}[Z_1|X, T] = 0.5$ .

Let  $C_4$ , a different data-generating process be as follows

$$X \sim \mathbb{1}(\mathcal{U} < 0.5)$$

$$T \sim \text{Bern}(2X)$$

$$Z_2 \sim \mathcal{N}(0.5, 1)$$

$$Y_2 \sim X + T + Z_2 - \mathbb{E}[Z_2|X, T] + \epsilon, \epsilon \sim \mathcal{N}(0, 1)$$

where  $\mathbb{E}[Z_2|X, T] = 0.5$ .

From the above we can show that both data generating processes have the same marginal distribution  $P(Y|T, X)$ .

$$\begin{aligned} P(Y_1|T, X) &= \mathbb{E}_{Z_1}[Y_1|T, X, Z_1] = \mathbb{E}[X + T + \mathbb{E}[Z_1] - \mathbb{E}[Z_1|X, T] + \epsilon] \\ &= \mathbb{E}[X + T + \epsilon] \end{aligned}$$

$$\begin{aligned} P(Y_2|T, X) &= \mathbb{E}_{Z_2}[Y_2|T, X, Z_2] = \mathbb{E}[X + T + \mathbb{E}[Z_2] - \mathbb{E}[Z_2|X, T] + \epsilon] \\ &= \mathbb{E}[X + T + \epsilon] \end{aligned}$$

As the marginal distribution is the same, and the average treatment effect is a deterministic function of expectations, the ATEs for both causal models converge to the same value.

□

## C Generative methods

In this section, we summarize the generative methods explored in this paper: Credence [Parikh et al., 2022], Realcause [Neal et al., 2020], and FrugalFlows [de Vassimon Manela et al., 2024]. While all aim to generate synthetic datasets that closely resemble the source data distribution, they differ in how they model the joint distribution  $P(X, T, Y)$ , the architectures they use, their training objectives, and the user-defined DGP parameters they support. We outline these differences below.

**Credence** Credence models the joint distribution as  $P(X, T, Y) = P(T) \cdot P(X | T) \cdot P(Y | X, T)$  using conditional variational autoencoders (cVAEs). cVAEs encode the data into a latent space modeled by a user-defined distribution (normal or uniform) and recreates the data by sampling from a decoder that takes as input the latent variable as well as the variable being conditioned on. For binary treatment  $T$ ,  $P(T)$  is modeled as a Bernoulli distribution estimated from data, while  $P(X | T)$  and  $P(Y | X, T)$  are learned via the cVAE framework.

Credence supports two DGP parameters: treatment effect and selection bias (also representing unobserved confounding bias), which users define as functions of the covariates and treatment. These functions are incorporated into the loss through KL divergence to measure how closely the generated data matches the source, along with two regularization terms that enforce the specified DGP parameters, each controlled by a hyperparameter. This approach offers both benefits and drawbacks. On the one hand, the data guides the strength of enforcement: low regularization weights signal that the specified constraint is incompatible with the source data. On the other hand, users must manually specify multiple constraint values and retrain the model each time, making the process computationally expensive and less scalable.

**modified-Credence** We implement a variant of Credence that retains its original architecture (and set of implemented DGP parameters) but changes the factorization of the joint distribution. We factorize the data distribution as:  $P(X, T, Y) = P(X) \cdot P(T | X) \cdot P(Y | T, X)$ . This modification allows us to directly use the empirical distribution of covariates from the source data, avoiding the need to learn  $P(X)$  from scratch. However, it increases the complexity of modeling  $P(T | X)$  especially with high-dimensional covariates. In practice, we found this factorization often produced datasets that more closely resembled the source distribution, though not perfectly.

**Realcause** Realcause models the joint distribution of the source data using the same factorization as our modified Credence:  $P(X, T, Y) = P(X) \cdot P(T | X) \cdot P(Y | T, X)$ . It uses separate MLP or flow networks to model each marginal and conditional distribution. This structure preserves the empirical covariate distribution from the source data. Unlike Credence, Realcause adopts the TARNET Shalit et al. [2017] architecture by learning two distinct models for the outcome:  $P(Y | T = 1, X)$ ,  $P(Y | T = 0, X)$  which helps maintain treatment relevance in high-dimensional settings where the model might otherwise ignore  $T$ .

Realcause supports three user-defined DGP parameters: positivity (overlap), treatment effect heterogeneity, and the scale of the causal effect. These DGP parameters are applied as post-hoc transformations to the generated data, allowing a single trained model to be reused for multiple configurations by adjusting parameters that shift or scale the output. However, Realcause does not support the simulation of unobserved confounding.

**FrugalFlows** FrugalFlows factorizes the joint distribution as the product of variationally independent distributions:  $P(T, X) \cdot P(Y | \text{do}(T)) \cdot \phi(Y, X)$ . Here,  $P(T, X)$  is the distribution of the ‘past’,  $P(Y | \text{do}(T))$  is the causal effect distribution and the  $\phi(Y, X)$  encodes the dependence (or correlation) between outcomes and covariates. The model learns each component using normalizing flows and enforces their dependence using copulas. Unlike other generative methods, FrugalFlows generates only causal outcomes  $Y$  and does not simulate counterfactuals.

FrugalFlows supports three DGP parameters: causal effect scale, unobserved confounding, and treatment effect heterogeneity. It incorporates these either through priors or post-hoc transformations, depending on the specific DGP parameter. This approach offers stronger enforcement of constraints since they directly shape the data generation process. However, overly strict specification can lead to distortions that push the generated data away from the source distribution.

## D SBICE: Algorithm and Experimental details

We present the full algorithmic procedure to use SBICE to evaluate the sensitivity of a set of causal estimators in Algorithm 1. We provide a pseudocode description of the SMC-ABC algorithm, and point to the original paper for details [Toni and Stumpf, 2010].

We implement SMC-ABC using the Python library pyABC Schälte et al. [2022]. The hyperparameter and algorithmic choices required to run SMC-ABC are outlined in Table 5. All of our experiments were run on a HPC cluster with distributed samplers to make sampling of datasets from the simulator more efficient.

We used the following set of causal estimators in our experiments.

1. X-Learner [Künzel et al., 2019]: A meta-learner algorithm to estimate the average treatment effect using two different underlying function: Linear regression (referred to as X (Lin)) and Gradient Boosted Trees (referred to as X (GBT)). We used the implementation in the EconML [Battocchi et al., 2019] package.
2. Double machine learning (DML) [Chernozhukov et al., 2019]: An algorithm that constructs a de-biased estimator of the causal parameter by using two models to estimate the residual errors. We used the implementation in the EconML python package, and used two learners: Linear regression (DML (Lin)) and Gradient Boosted Trees (DML (GBT)).
3. Doubly robust (DR) [Dudík et al., 2014]: This estimator combines two models: one for outcome regression and another for the treatment (propensity score) to estimate the causal effect. The advantage of using this estimator is that the effect is unbiased if either model is correctly specified. We use the implementation in the EconML package and use a linear model for both the treatment and outcome functions (DR (Lin)).
4. Causal BART [Hill, 2011]: This estimator leverages Bayesian Additive Regression Trees (BART) to estimate the causal effect. We use its R implementation [Dorie et al., 2025] in our experiments.
5. Targeted Maximum Likelihood Estimator (TMLE) [Van Der Laan and Rubin, 2006]: We use the implementation of TMLE as described in the package zEpid Zivich et al. [2022].

---

**Algorithm 1:** SBICE: Simulation-based inference for causal evaluation

---

**Input:** Source dataset  $D = \{\mathbf{X}, T, Y\}$ ;  
Prior over knobs  $p(\boldsymbol{\theta})$ ;  
Causal estimators  $\mathcal{M}$   
**Output:** Posterior datasets  $\mathcal{D}$ ;  
Causal estimates  $\mathcal{M}(\mathcal{D})$

- 1 Train simulator  $f(D; \boldsymbol{\theta})$  using source dataset  $D$ ;
- 2 Define prior  $p(\boldsymbol{\theta})$ ;
- 3 Define distance function  $d(x, D)$  (e.g., Sliced Wasserstein);
- 4 Set tolerance schedule  $\epsilon_1 > \epsilon_2 > \dots \epsilon_m \geq 0$ , and iteration index  $i \leftarrow 0$ ;
- 5 **Procedure** *SMC-ABC*:
- 6   **while**  $i < m$  or  $|\mathcal{D}_{\text{sim}}| < M$  **do**
- 7     // Sample  $M$  accepted datasets
- 8     Sample  $\theta \sim p(\boldsymbol{\theta})$ ;
- 9     Generate  $x \sim f(D; \theta)$ ;
- 10    **if**  $d(x, D) < \epsilon$  **then**
- 11     Add  $x$  to accepted set  $\mathcal{D}_{\text{sim}}$ ;
- 12     Set new tolerance  $\epsilon = \epsilon_{i+1}$
- 13    // Resample and perturb
- 14    **foreach**  $x' \in \mathcal{D}_{\text{sim}}$  **do**
- 15     Perturb:  $x'' \sim K(x | x')$ ;
- 16     **if**  $d(x'', D) < \epsilon$  **then**
- 17      Add  $x'$  to accepted set  $\mathcal{D}_{\text{sim}}$ ;
- 18    Update  $\epsilon$ ;
- 19   **return**  $P(\boldsymbol{\theta} | D)$
- 20 Run SMC-ABC to obtain posterior  $P(\boldsymbol{\theta} | D)$ ;
- 21 Sample posterior datasets  $\mathcal{D} \sim f(D; \theta)$  using  $\theta \sim P(\boldsymbol{\theta} | D)$ ;
- 22 Compute causal estimates:  $\mathcal{M}(\mathcal{D})$ ;

---

Table 5: Hyperparameters and Implementation choices for SMC-ABC.

Hyperparameter	Range of values
Maximum number of iterations	[12, 15]
Minimum epsilon threshold	[0.001, 0.005]
Distance metric	Sliced-Wasserstein (L2 norm; 100 projections)

## E Evaluating SBICE on synthetic datasets generated using parametric data-generating processes

We evaluate SBICE on a suite of synthetic datasets generated from simple, parametric data-generating processes. These experiments assess when the inferred posterior yields more informative datasets than those generated by sampling from the prior. We systematically vary characteristics of the data-generating process and simulator by introducing model misspecification, using non-identifiable and partially identifiable DGP parameters. We label the synthetic datasets generated in this manner as LinearParam DGP( $x$ ), with  $x$  being the experiment identifier.

For each experiment, we specify the data-generating process, simulator design, set of DGP parameters, and user-defined prior. To evaluate SBICE, we compute the classifier AUC between source data and datasets sampled from the posterior and prior distributions, where lower AUC indicates closer alignment with the source. We also measure the bias squared error (BSE) of several causal estimators applied to these datasets, with lower values indicating better fidelity to the source distribution.

### E.1 LinearParam Sim1: Linear, parametric data-generating process and simulator

In this setting, we consider a linear, parametric data generating process (DGP) involving a single unobserved confounder  $Z$ , an observed confounder  $X$ , a binary treatment  $T$ , and a continuous outcome  $Y$ .

#### LinearParam DGP1

$$\begin{aligned} Z &\sim \mathcal{N}(0, 1) \\ X &\sim \mathcal{N}(0, 1) \\ T &\sim \text{Binomial}(\rho Z + \beta X + \mathcal{N}(0, 0.1)) \\ Y &= \rho Z + \beta X + \tau T + \mathcal{N}(0, 0.1) \end{aligned} \quad (2)$$

We assume that the simulator is correctly specified, i.e., it closely matches the data generating process.

#### LinearParam Sim1

$$\begin{aligned} Z &\sim \mathcal{N}(0, 1) \\ X &= X \\ T &\sim \text{Binomial}(\rho Z + \beta X + \mathcal{N}(0, 0.1)) \\ Y &= \rho Z + \beta X + \tau T + \mathcal{N}(0, 0.1) \end{aligned} \quad (3)$$

This setting has three DGP parameters:  $\rho$  (unobserved confounding),  $\beta$  (observed confounding), and  $\tau$  (causal effect). We assume that they are independent and therefore use uniform, non-overlapping priors for them. The true parameter values used in the DGP are  $\rho = 1.0$ ,  $\beta = -1.5$ , and  $\tau = 1.5$ .

#### Prior

$$\begin{aligned} \text{Prior}(\rho) &\sim U[0.0, 2.0] \\ \text{Prior}(\beta) &\sim U[-2.0, 1.0] \\ \text{Prior}(\tau) &\sim U[0.0, 2.0] \end{aligned} \quad (4)$$

We generate three sets of 50 datasets each:

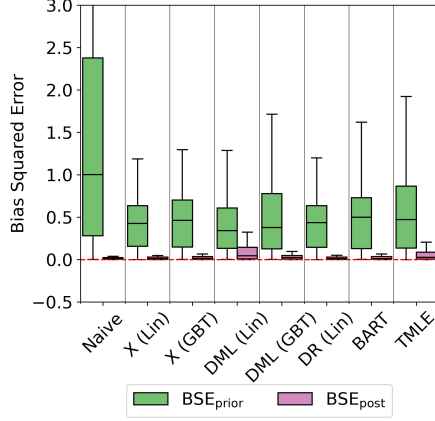
1. **Source datasets** from the true DGP: LinearParam DGP1,
2. **Posterior datasets** using parameter samples from the posterior distribution, and
3. **Prior datasets** using parameter samples from the prior.

**Evaluation** We report the mean classifier AUCs for the posterior and prior datasets in Table 5. We plot the bias of the causal estimators for the posterior, prior and source datasets in Figure 5. We also plot the posterior distribution for each of the DGP parameters in Figure 6. For this setting, we find that SBICE improves posterior estimates and that posterior datasets are informative of the performance of causal estimators.

### E.2 Misspecified simulators

However, in real-world applications, the true data generating process (DGP) is typically unknown, and the simulator specified by the researcher may be misspecified. To understand the effects of such misspecification in parameterized linear models, we investigate how different types of model mismatch influence the estimated posterior distribution and subsequent performance of causal estimators. We consider several categories of misspecification, including variations in the form of unobserved confounding, increased noise levels, linear approximations to nonlinear functions, and the inclusion of interaction terms. Each variant of the DGP and its corresponding simulator is described below.

**LinearParam Sim2: Noisy simulator** In this setting, we examine the effect of additive, Gaussian noise to the outcome model within the simulator. We use the same DGP as before: LinearParam DGP1, but use the simulator LinearParam Sim2 described below. The true parameter values are  $\rho = 1.0$ ,  $\beta = -1.5$ , and  $\tau = 1.5$ .



	Prior	Posterior
AUC	$0.77 \pm 0.13$	$0.50 \pm 0.01$
<b>Mean BSE</b>		
Diff. of Means	1.382	0.018
X (Lin)	0.575	0.015
X (GBT)	0.587	0.020
DML (Lin)	0.551	0.083
DML (GBT)	0.564	0.028
DR (Lin)	8e5	0.016
BART	0.590	0.018
TMLE	0.624	0.065

Figure 5: Classifier AUC and Mean BSE of causal estimators for DGP: LinearParam DGP1 and Simulator: LinearParam Sim1.

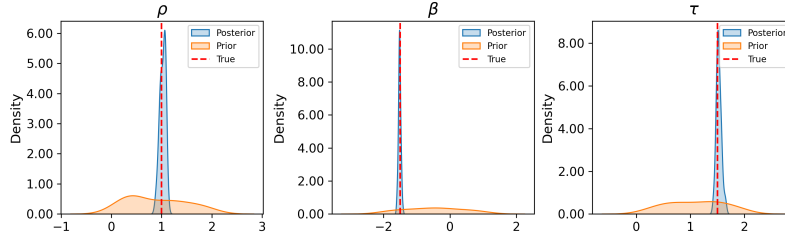


Figure 6: Posterior distribution for DGP: LinearParam DGP1, Simulator: LinearParam Sim1

### LinearParam Sim2

$$\begin{aligned}
 Z &\sim \mathcal{N}(0, 1) \\
 X &= X \\
 T &\sim \text{Binomial}(\rho Z + \beta X + \mathcal{N}(0, 0.1)) \\
 Y &= \rho Z + \beta X + \tau T + \mathcal{N}(0, \mathbf{1.0})
 \end{aligned} \tag{5}$$

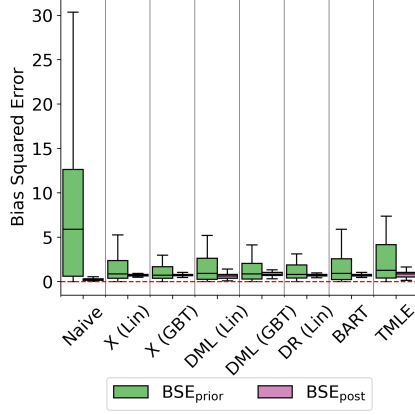
### Prior

$$\begin{aligned}
 \text{Prior}(\rho) &\sim U[-5.0, 5.0] \\
 \text{Prior}(\beta) &\sim U[-5.0, 5.0] \\
 \text{Prior}(\tau) &\sim U[-5.0, 5.0]
 \end{aligned} \tag{6}$$

**Evaluation** We present the results of our evaluation for this setting in Figures 7 and 8. We find that despite the noisy simulator, the BSE of the posterior estimates is lower compared to the prior, highlighting the robustness of SBICE to moderate misspecification.

**LinearParam Sim3: Misspecified unobserved confounder ( $Z$ )** In this setting, we investigate the effect of misspecifying the distribution of the unobserved confounder  $Z$ . We use LinearParam DGP1 as the data-generating process but misspecify the distribution of the unobserved confounder  $Z$ . The true parameters are  $\rho = 1.0$ ,  $\beta = -1.5$ , and  $\tau = 1.5$ . We use the same priors as in Linear Sim2 (Equation 6).

The unobserved confounder  $Z$  is modeled using an exponential distribution rather than the true Gaussian distribution.



	Prior	Posterior
AUC	0.9±0.06	0.53±0.01
<b>Mean BSE</b>		
Diff. of Means	8.964	0.237
X (Lin)	1.568	0.720
X (GBT)	1.324	0.740
DML (Lin)	1.815	0.660
DML (GBT)	1.847	0.847
DR (Lin)	1.520	0.729
BART	1.699	0.728
TMLE	5.069	0.843

Figure 7: Classifier AUC and Mean BSE of causal estimators for DGP: LinearParam DGP1 and Simulator: LinearParam Sim2.

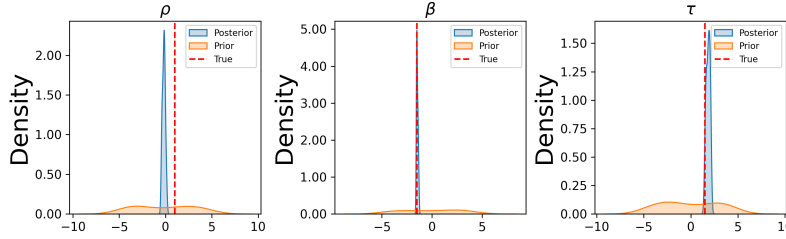


Figure 8: Posterior distribution for DGP: LinearParam DGP1, Simulator: LinearParam Sim2

### LinearParam Sim3

$$\begin{aligned}
 Z &\sim \text{Exponential}(0.5) \\
 X &= X \\
 T &\sim \text{Binomial}(\rho Z + \beta X + \mathcal{N}(0, 0.1)) \\
 Y &= \rho Z + \beta X + \tau T + \mathcal{N}(0, 0.1)
 \end{aligned} \tag{7}$$

**Evaluation** This experiment evaluates the robustness of SBICE when the unobserved confounder deviates substantially from the assumed distribution. Notably, in this setting, the posterior distribution over  $\rho$  concentrates near zero (see Figure 10), effectively down-weighting the influence of the misspecified confounder in order to better match the source data distribution. Figure 9 illustrates the estimator bias and the posterior/prior distributions over parameters. This example highlights the reason to consider both the classifier AUC score and the BSE to evaluate the posterior. The mean BSE for the posterior estimates remain low, as the variance of the posterior distribution is low.

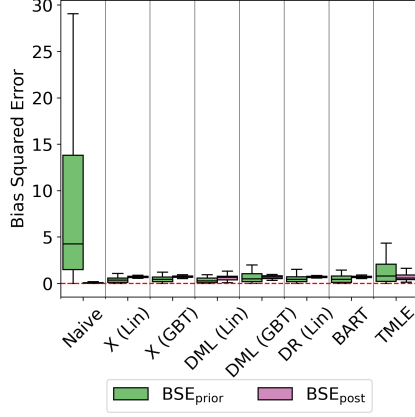
**LinearParam Sim4: Misspecified simulator with additional interaction terms** In this setting, we explore the impact of misspecifying the functional form of the simulator by introducing an interaction term between the observed and unobserved confounders,  $X$  and  $Z$ . The true parameter values and prior distributions are identical to those used with LinearParam Sim2 (Equation 6). The simulator is defined as follows.

### LinearParam Sim4

$$\begin{aligned}
 Z &\sim \mathcal{N}(0, 1) \\
 X &= X \\
 T &\sim \text{Binomial}(\rho Z + \beta X + X \cdot Z + \mathcal{N}(0, 0.1)) \\
 Y &= \rho Z + \beta X + \tau T + X \cdot Z + \mathcal{N}(0, 0.1)
 \end{aligned} \tag{8}$$

**Evaluation** The interaction term  $X \cdot Z$ , which is absent in the true DGP (LinearParam DGP1), introduces a form of structural misspecification in both the treatment and outcome models of the





	Prior	Posterior
AUC	$0.93 \pm 0.06$	$0.89 \pm 0.02$
<b>Mean BSE</b>		
Diff. of Means	8.984	0.072
X (Lin)	0.491	0.709
X (GBT)	0.614	0.728
DML (Lin)	0.474	0.642
DML (GBT)	1.709	0.691
DR (Lin)	30.894	0.715
BART	0.805	0.722
TMLE	2.310	0.693

Figure 9: Classifier AUC and Mean BSE of causal estimators for DGP: LinearParam DGP1 and Simulator: LinearParam Sim3.

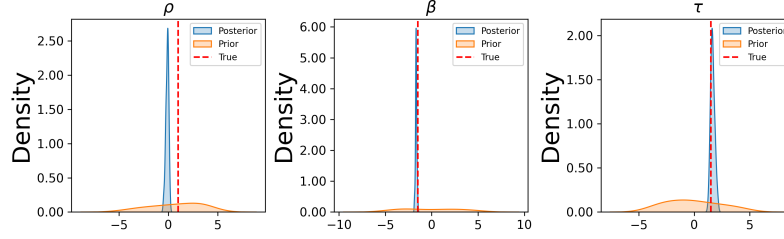
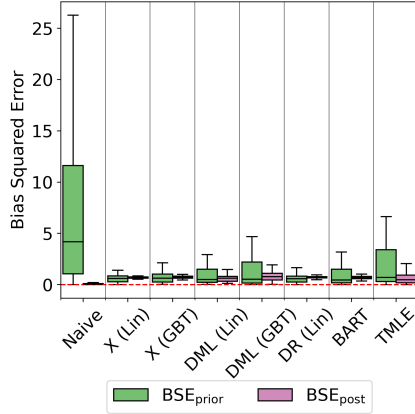


Figure 10: Posterior distribution for DGP: LinearParam DGP1, Simulator: LinearParam Sim3

simulator. Figure 11 displays the results. Despite the added complexity, SBICE is able to adjust for the mismatch to some extent by adapting the posterior over  $\theta$ , though some deviation in estimator bias for the posterior datasets remains due to the unmodeled interaction. We include the posterior distribution in Figure 12.



	Prior	Posterior
AUC	$0.97 \pm 0.03$	$0.85 \pm 0.01$
<b>Mean BSE</b>		
Diff. of Means	8.375	0.079
X (Lin)	1.212	0.700
X (GBT)	1.142	0.724
DML (Lin)	1.313	0.633
DML (GBT)	2.407	0.858
DR (Lin)	1.148	0.731
BART	1.222	0.680
TMLE	2.362	0.688

Figure 11: Classifier AUC and Mean BSE of causal estimators for DGP: LinearParam DGP1 and Simulator: LinearParam Sim4.

**LinearParam Sim5: Misspecified simulator with linear outcome function** In this setting, we explore a structural mismatch where the true outcome function is nonlinear—specifically, a polynomial function of the covariates and treatment—while the simulator assumes a linear relationship. This setup reflects a common form of model misspecification in applied settings, where complex

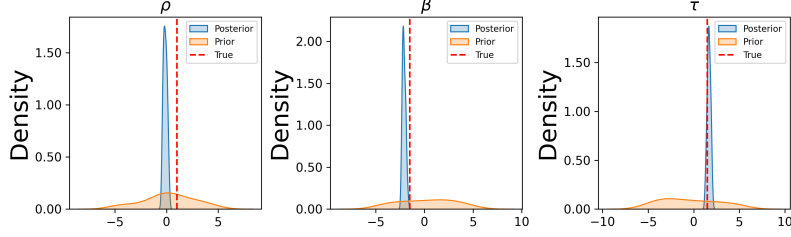


Figure 12: Posterior distribution for DGP: LinearParam DGP1, Simulator: LinearParam Sim4

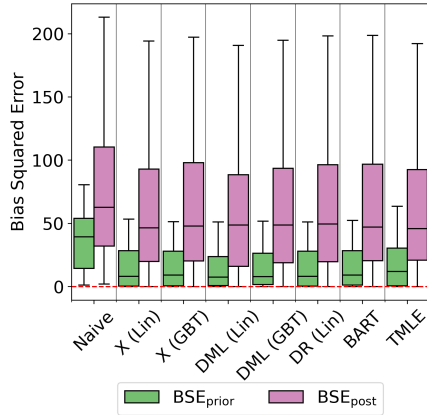
interactions or nonlinearities in the data are simplified in simulation. The true DGP is defined as follows.

### LinearParam DGP5

$$\begin{aligned}
 Z &\sim \mathcal{N}(0, 1) \\
 X &\sim \mathcal{N}(0, 1) \\
 T &\sim \text{Binomial}(\rho Z + \beta X + \mathcal{N}(0, 0.1)) \\
 Y &= \rho(Z^2 + Z \cdot X) + \beta(X^2 - X \cdot T) + \tau T + \mathcal{N}(0, 0.1)
 \end{aligned} \tag{9}$$

The simulator, by contrast, is the same as LinearParam Sim1 (Equation 3), and does not capture the true polynomial structure of the outcome. The true parameter values and uniform priors remain the same as in LinearParam Sim2 (Equation 6). This experiment allows us to evaluate how well SBICE handles misspecification arising from oversimplified functional forms in the simulator.

**Evaluation** The results are shown in Figures 13 and 14, which compares estimator bias and parameter distributions for datasets generated from the posterior and prior. In this setting, we find that both the posterior and prior estimates are different compared to the source distribution (indicated by the high BSE) and high variance across all estimates. We also find that SBICE is unable to recover the true parameters from the data.



	Prior	Posterior
AUC	0.93±0.04	0.9±0.02
<b>Mean BSE</b>		
Diff. of Means	37.990	77.401
X (Lin)	15.124	62.779
X (GBT)	15.722	63.065
DML (Lin)	13.822	62.020
DML (GBT)	16.163	63.475
DR (Lin)	8e6	62.929
BART	16.416	63.297
TMLE	18.377	62.499

Figure 13: Classifier AUC and Mean BSE of causal estimators for DGP: LinearParam DGP5 and Simulator: LinearParam Sim1.

**Key takeaway:** With misspecified simulators, the causal estimates on posterior datasets do not align with the source data—sometimes performing worse than the prior—depending on the nature of the misspecification. This highlights the importance of using flexible simulators that can accurately capture the source data distribution and independently vary the DGP parameters during simulation. Such flexibility is crucial for ensuring meaningful inference under misspecification.

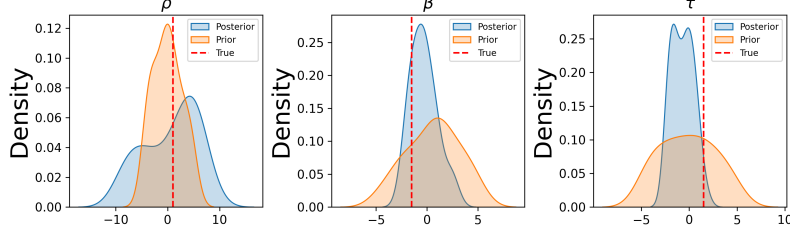


Figure 14: Posterior distribution for DGP: LinearParam DGP5, Simulator: LinearParam Sim1

### E.3 Non-identifiable parameters

We analyze the cases where the observed data distribution provides no information about the values of DGP parameters.

**LinearParam Sim6: Non-identifiable parameters from observed data** In this setting, we constrain the sum of two parameters:  $\rho, \tau$ . This leads to a fundamental non-identifiability in the model. In this formulation,  $T$  is deterministically derived from  $Z$  and a uniform random noise term. As a result, the joint distribution of  $(T, Y)$  remains invariant for any pair of values  $(\rho, \tau)$  such that their sum  $\rho + \tau = c$  is constant. While individual values of  $\rho$  and  $\tau$  are not identifiable from the data, their sum is identifiable. Consequently, any prior over  $\rho$  and  $\tau$  that maintains a constant sum will yield a posterior distribution that is also uniform across that constraint. The data generating process is described below.

#### LinearParam DGP6

$$\begin{aligned} Z &\sim \text{Binomial}(0.5) \\ X &\sim \mathcal{N}(0, 1) \\ T &= \mathbb{1}(Z + U[0, 0.5)) \\ Y &= \rho Z + \beta X + \tau T + U[0, 0.5) \end{aligned} \tag{10}$$

We assume that the simulator is correctly specified and matches the structure of the true DGP. The true parameters are  $\rho = 2.0$ ,  $\beta = 0.5$ , and  $\tau = 2.0$ . The simulator is specified as:

#### LinearParam Sim6

$$\begin{aligned} Z &\sim \text{Binomial}(0.5) \\ X &= X \\ T &= \mathbb{1}(Z + U[0, 0.5)) \\ Y &= \rho Z + \beta X + \tau T + U[0, 0.5) \end{aligned} \tag{11}$$

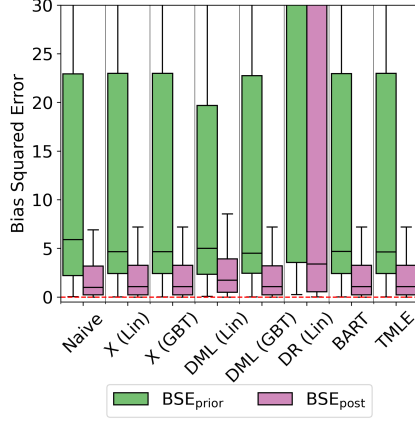
We use uniform, independent priors over all three parameters:

#### Prior

$$\begin{aligned} \text{Prior}(\rho) &\sim U[0.0, 10.0] \\ \text{Prior}(\beta) &\sim U[0.0, 10.0] \\ \text{Prior}(\tau) &\sim U[0.0, 10.0] \end{aligned} \tag{12}$$

**Evaluation** This setup allows us to analyze the implications of parameter non-identifiability on the posterior distributions and causal estimator performance. Figure 15 displays the BSE and the classifier AUC for posterior and prior datasets. Despite the non-identifiability, the posterior estimates are similar to the source estimates as we still have information on  $\beta$  learned from the source data. The posterior also converges to a distribution of values such that the sum of  $\rho + \tau$  is a constant. This distribution is displayed in Figure 16.

**LinearParam Sim7: Using joint priors with constrained sum** We revisit the non-identifiability scenario from LinearParam Sim6 with a key modification: instead of using independent priors over  $\rho$  and  $\tau$ , we impose a joint prior distribution that explicitly enforces the constraint  $\rho + \tau = c$ , where



	Prior	Posterior
AUC	0.99±0.03	0.52±0.02
<b>Mean BSE</b>		
Diff. of Means	15.952	2.040
X (Lin)	16.078	2.054
X (GBT)	16.081	2.055
DML (Lin)	14.988	2.723
DML (GBT)	15.894	2.048
DR (Lin)	1e6	1e6
BART	16.085	2.054
TMLE	16.081	2.054

Figure 15: Classifier AUC and Mean BSE of causal estimators for DGP: LinearParam DGP6 and Simulator: LinearParam Sim6.

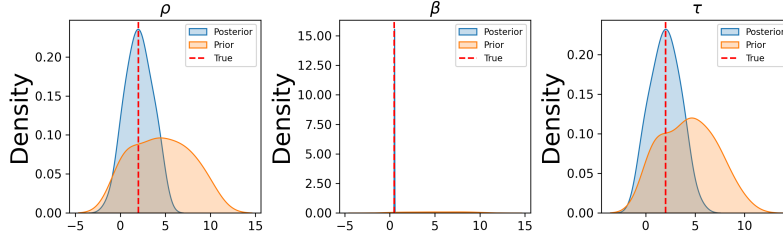


Figure 16: Posterior distribution for DGP: LinearParam DGP6, Simulator: LinearParam Sim6

$c$  is a known, user-specified constant. This reflects a setting in which the researcher has domain knowledge about the functional relationship between parameters, even if the individual values remain unknown.

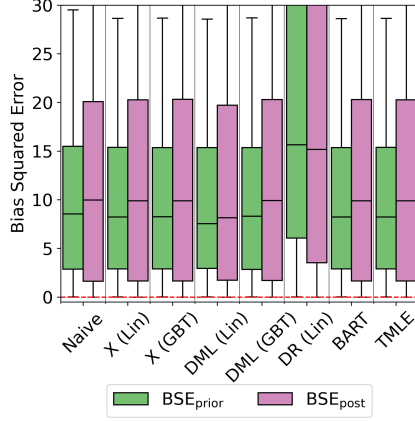
Our hypothesis is that under this constraint, the posterior and prior datasets may exhibit similar behavior, as both are restricted to lie on the same manifold in parameter space. Consequently, any observed differences can be primarily attributed to better posterior estimation of the identifiable parameter  $\beta$ . The true parameter values used to generated the observed data are  $\rho = 1.0, \beta = 0.3, \tau = 2.0$ . The joint prior is defined as follows.

#### Prior

$$\begin{aligned}
 \text{Prior}(\rho) &\sim U[-5.0, 5.0] \\
 \text{Prior}(\beta) &\sim U[0.0, 5.0] \\
 \text{Prior}(\tau) &\sim U[-20.0, 20.0] \\
 \text{Constraint: } \rho + \tau &= c, c = 3.0
 \end{aligned} \tag{13}$$

Formally, the joint prior distribution over  $(\rho, \tau)$  is defined as  $P(\rho, \tau) = P(\rho) \cdot P(\tau)$  iff  $\rho + \tau = c$  else  $P(\rho, \tau) = 0$ . During simulation, we sample values for  $\rho$  from its marginal prior and determine  $\tau$  accordingly to satisfy the constraint. The classifier AUC and mean BSE in this setting is visualized in Figure 17 and 18.

Contrary to our initial hypothesis, imposing a joint prior that enforces a known relationship between parameters does not lead to a more informative posterior. Instead, we find that the constraint restricts the flexibility of the posterior distribution, limiting its ability to align with the source data. Both the posterior and prior datasets exhibit high BSE across all estimators. These results suggest that, in scenarios with non-identifiable parameters, incorporating partial knowledge through hard constraints on the DGP parameters may hinder rather than help. It may be preferable to allow the inference process to explore a broader parameter space without such restrictions.



	Prior	Posterior
AUC	0.92±0.13	0.5±0.02
<b>Mean BSE</b>		
Diff. of Means	10.737	13.110
X (Lin)	10.860	13.120
X (GBT)	10.864	13.121
DML (Lin)	11.230	13.011
DML (GBT)	10.856	13.145
DR (Lin)	1e6	1e6
BART	10.856	13.122
TMLE	10.860	13.120

Figure 17: Classifier AUC and Mean BSE of causal estimators for DGP: LinearParam DGP6 and Simulator: LinearParam Sim7 (which is similar to Sim6 with updated prior distribution).

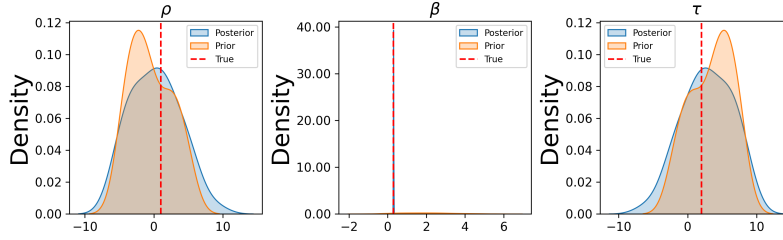


Figure 18: Posterior distribution for DGP: LinearParam DGP6, Simulator: LinearParam Sim7 (similar to LinearParam Sim6 with joint priors).

**LinearParam Sim8: Partial identifiability of parameters** Earlier, we examined a case where the parameters  $\rho$  and  $\tau$  were non-identifiable due to a symmetry in the data generating process (DGP): the treatment assignment depended solely on the unobserved confounder  $Z$ , and only the sum  $\rho + \tau$  could be inferred. To make the setting more realistic and address the identifiability issue, we now introduce a modified DGP where treatment  $T$  depends not only on  $Z$  but also on the observed covariate  $X$ . This modification helps break the symmetry and allows for partial identifiability of the individual parameters. The DGP is given by:

**LinearParam DGP8**

$$\begin{aligned}
 Z &\sim \text{Binomial}(0.5) \\
 X &\sim \mathcal{N}(0, 1) \\
 T &= \mathbb{1}(Z + 0.4X + U[0.0, 0.5]) \\
 Y &= \rho Z + \beta X + \tau T + U[0, 0.5]
 \end{aligned} \tag{14}$$

We use the following true parameter values:  $\rho = 1.0, \beta = 0.3, \tau = 2.0$ . The priors are uniform, independent random variables:

**Prior**

$$\begin{aligned}
 \text{Prior}(\rho) &\sim U[0.0, 10.0] \\
 \text{Prior}(\beta) &\sim U[0.0, 10.0] \\
 \text{Prior}(\tau) &\sim U[0.0, 10.0]
 \end{aligned} \tag{15}$$

**Evaluation** The inclusion of  $X$  as a predictor of  $T$  introduces additional variation that helps disambiguate the effects of  $\rho$  and  $\tau$ , making it easier to learn about these parameters from the observed data. The results of this experiment are shown in Figure 19 and 20.

By modifying the treatment assignment mechanism to include an observed covariate, we ensure that the dataset is informative for the values of the DGP parameters, and learn a posterior over  $\rho$

and  $\tau$ . As a result, we observe lower BSE for the posterior datasets. These results demonstrate that even small changes in the DGP that provide additional structure can lead to significantly more informative posteriors—highlighting the importance of leveraging partial identifiability when complete identification is not possible.

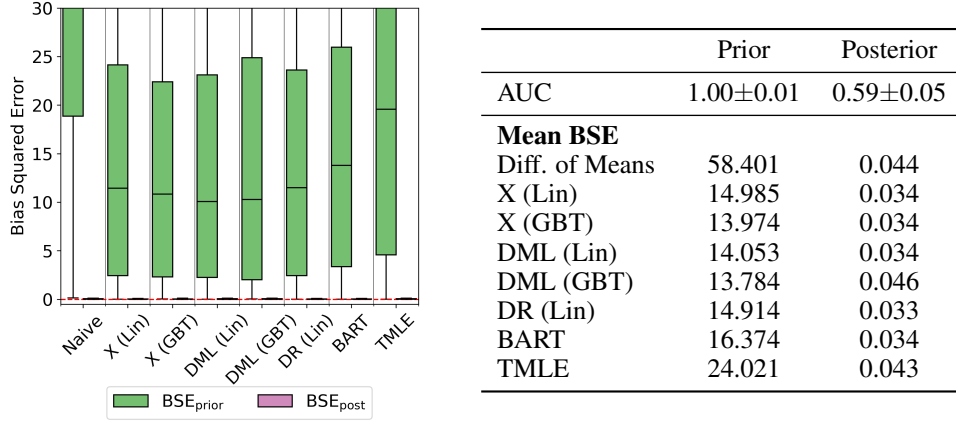


Figure 19: Classifier AUC and mean BSE of causal estimators for DGP: LinearParam DGP8 and Simulator: LinearParam Sim8 (which is similar to Sim6).

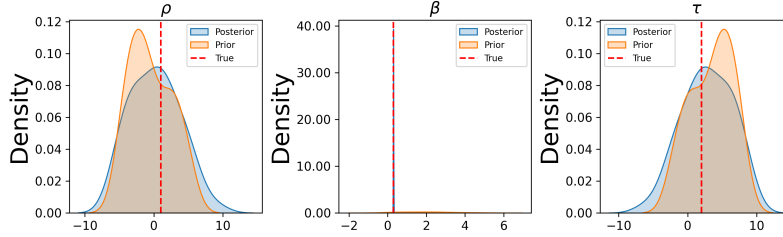


Figure 20: Posterior distribution for DGP: LinearParam DGP8, Simulator: LinearParam Sim8 (similar to LinearParam Sim6).

#### E.4 Misspecified prior distributions

In many real-world applications, domain knowledge about the underlying data-generating mechanisms may be limited or imprecise. As a result, prior distributions over simulator parameters can often be either too narrow or entirely misaligned with the true values. In this section, we explore such scenarios to better understand the consequences of using misspecified priors in causal estimation.

**LinearParam Sim9: Narrow priors** We begin with a scenario in which the prior distributions are relatively narrow but still include the true parameter values. These priors represent a situation where the researcher believes they have strong—but not necessarily perfect—knowledge about the plausible range of parameter values. We reuse the data-generating process from earlier, LinearParam DGP6, with a correctly specified simulator:

**LinearParam Sim9**

$$\begin{aligned}
 Z &\sim \text{Binomial}(0.5) \\
 X &\sim \mathcal{N}(0, 1) \\
 T &= \mathbb{1}(Z + U[0, 0.5)) \\
 Y &= \rho Z + \beta X + \tau T + U[0, 0.5)
 \end{aligned} \tag{16}$$

The true parameter values are  $\rho = 1.0, \beta = 0.3, \tau = 1.0$ . We assume independent uniform priors over a narrow range:

## Prior

$$\begin{aligned}\text{Prior}(\rho) &\sim U[0.0, 2.0] \\ \text{Prior}(\beta) &\sim U[0.0, 2.0] \\ \text{Prior}(\tau) &\sim U[0.0, 2.0]\end{aligned}\tag{17}$$

**Evaluation** Our hypothesis is that because the priors are informative and centered near the true values, the posterior will not offer a substantial improvement in the quality of datasets or causal estimates. The posterior and prior should lead to similar estimator performance. This hypothesis is confirmed by the results shown in Figure 21 and 22, where both the posterior and prior samples yield comparable ATE bias and parameter distributions.

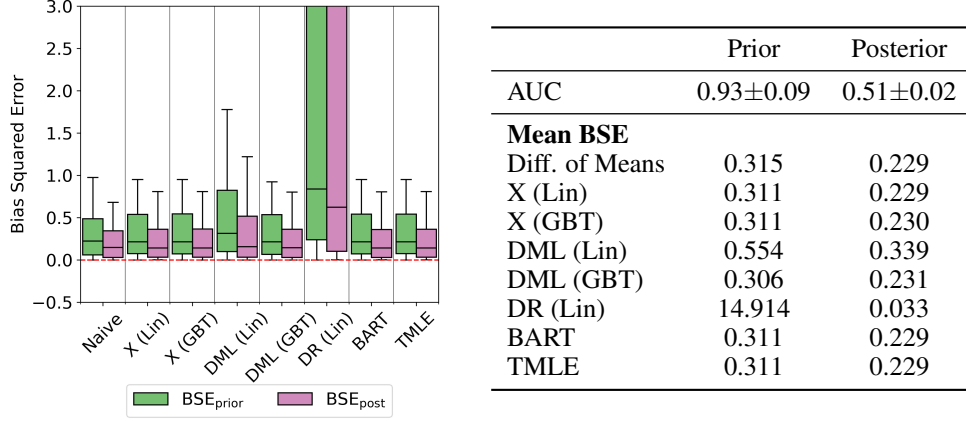


Figure 21: Classifier AUC and Mean BSE of causal estimators for DGP: LinearParam DGP6 and Simulator: LinearParam Sim9.

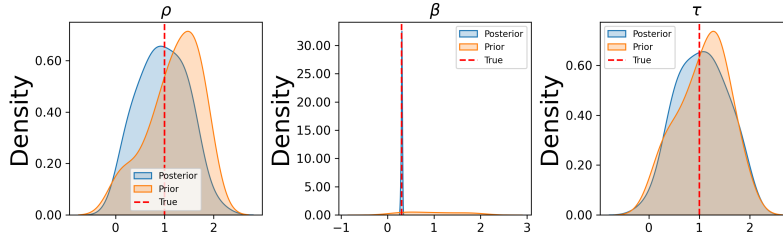


Figure 22: Posterior distribution for DGP: LinearParam DGP6, Simulator: LinearParam Sim9

**LinearParam Sim10: ‘Incorrect’ priors** In practical scenarios, it is not uncommon to misspecify the range or directionality of plausible parameter values due to limited or misleading prior knowledge. This setting examines such cases where the prior distributions do not contain the true values of the DGP parameters that generated the observed data. When this occurs, we hypothesize that the posterior distribution does not converge toward the true parameter values, but instead toward those that produce simulations whose distributions are closest to the source data, as measured by a discrepancy metric—here, the sliced-Wasserstein distance.

To test this hypothesis, we run a controlled experiment with a linear, parametric simulator. The data-generating process (DGP) LinearParam DGP10 is defined as:

## LinearParam DGP10

$$\begin{aligned}Z &\sim \mathcal{N}(0, 1) \\ X &\sim \mathcal{N}(0, 1) \\ T &\sim \text{Binomial}(\rho Z + \beta X + \mathcal{N}(0, 0.1)) \\ Y &= \rho Z + \beta X + \tau T + \mathcal{N}(0, 0.1)\end{aligned}\tag{18}$$

The true values of the DGP parameters are  $\rho = 1.0, \beta = -1.5, \tau = 1.5$ . However, the priors are intentionally misspecified, such that none of the true values fall within their support:

### Prior

$$\begin{aligned} \text{Prior}(\rho) &\sim U[-2.0, 0.0] \\ \text{Prior}(\beta) &\sim U[0.0, 2.0] \\ \text{Prior}(\tau) &\sim U[-2.0, 0.0] \end{aligned} \tag{19}$$

**Evaluation** The resulting mean BSE and classifier AUC as well as the posterior distributions are presented in Figures 23 and 24. We note that the posterior and prior exhibit similar performance across estimators.

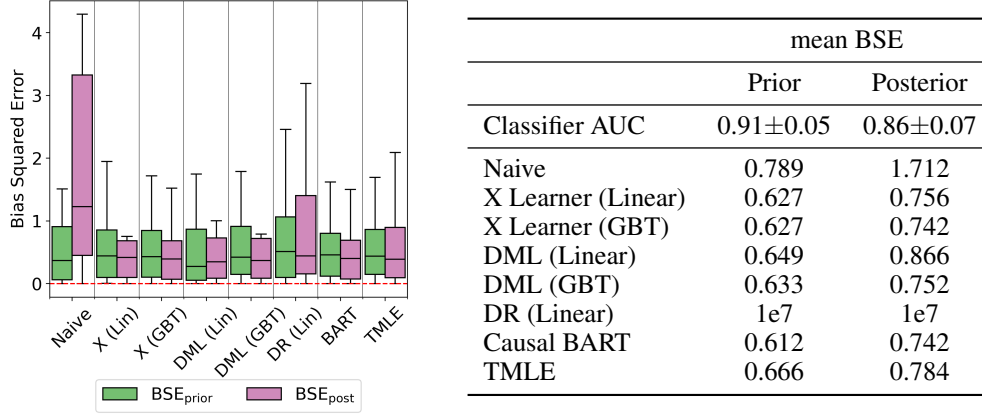


Figure 23: Classifier AUC and Mean BSE of causal estimators for DGP: LinearParam DGP10 and Simulator: LinearParam Sim10.

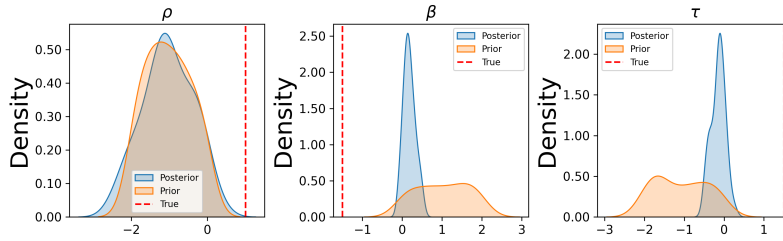


Figure 24: Posterior distribution for DGP: LinearParam DGP10, Simulator: LinearParam Sim10

The specification of priors—and their potential misspecification—is a long-standing consideration in the Bayesian literature. While identifying the correct prior is often impractical, we recommend that practitioners using this framework iterate over a range of plausible prior distributions and manually inspect the datasets generated by the simulator. This process can surface misalignments between prior assumptions and observable data. As a practical guideline, we suggest beginning with heavy-tailed and broad priors to allow the posterior more flexibility during the initial exploration



### Key takeaway

Using parametric, linear simulators we explored how different sources of uncertainty and modeling choices impact the effectiveness of SBICE.

- **Flexible simulators:** Even when the true functional form deviates from the simulator’s assumptions (e.g., added interaction or non-linear terms), the method remains robust as long as the simulator is expressive enough to capture distributional similarities. In these cases, the causal estimates on posterior datasets mirrored that of the source data.
- **Well-calibrated, wide priors:** In settings with limited domain knowledge, wide priors with heavy tails allow the posterior to concentrate near plausible values. Even when the priors are misspecified, if the simulator is accurate and the posterior matching is distributionally guided (e.g., via sliced-Wasserstein distance), the resulting datasets often lead to informative posteriors.
- **Low model misspecification:** In parametric settings where the simulator closely matches the true DGP, the method reliably sharpens inference. Posterior datasets exhibit lower bias squared error and classifier AUC.
- **Joint posterior estimation for identifiable subspaces:** When parameters are non-identifiable individually but have identifiable combinations (e.g., fixed sum constraints), the method can still recover meaningful structure when the remaining parameters (like  $\beta$ ) are well-informed by the data.

We summarize the classifier AUC for all the settings described above in Table 6.

Table 6: Classifier AUC of the posterior and prior datasets when compared to the source datasets for all settings.

Setting	Classifier AUC	
	Prior	Posterior
Linear, parametric	$0.77 \pm 0.13$	$0.50 \pm 0.01$
Misspecified simulator (noisy)	$0.90 \pm 0.06$	$0.53 \pm 0.01$
Misspecified simulator (Z)	$0.93 \pm 0.06$	$0.89 \pm 0.02$
Misspecified simulator (interaction terms)	$0.93 \pm 0.03$	$0.85 \pm 0.01$
Misspecified simulator (linear approximation)	$0.93 \pm 0.04$	$0.90 \pm 0.02$
Non-identifiable parameters	$0.96 \pm 0.06$	$0.52 \pm 0.01$
Non-identifiable parameters (joint priors, known sum)	$0.99 \pm 0.03$	$0.52 \pm 0.02$
Partially identifiable parameters	$0.92 \pm 0.13$	$0.50 \pm 0.02$
Narrow priors	$0.93 \pm 0.09$	$0.51 \pm 0.02$
Incorrect priors	$0.91 \pm 0.05$	$0.86 \pm 0.07$

## F Evaluating SBICE on synthetic datasets generated using non-parametric data-generating processes

We evaluate SBICE on synthetic datasets with high-dimensional covariates, generated using parametric models and frugal parameterization [Evans and Didelez, 2024]. For each experiment, we report classifier AUC and mean BSE for a set of causal estimators. These metrics assess how closely the generated datasets resemble the source distribution and how the inferred posterior affects estimator performance. For these datasets, we vary observable characteristics, including sample size, number of covariates and functional relationships between variables.

We use two types of simulators for these experiments: (1) **FrugalParam**, which implements the data-generating process directly via frugal parameterization and serves as a correctly specified simulator; and (2) **FrugalFlows** [de Vassimon Manela et al., 2024], a non-parametric simulator based on normalizing flows and copulas. Note that the FrugalFlows simulators may not be able to accurately learn the source data distribution as they require large sample sizes for convergence. We use the labels Frugal DGP( $x$ ) to denote these types of datasets.

### F.1 Frugal DGP1

**Frugal DGP1** This dataset includes two unobserved confounders  $Z_1, Z_2$ , and three observed confounders  $X_1, X_2, X_3$ , a binary treatment  $T$  and outcome  $Y$ . We generate 3000 samples from the following causal model.

$$\begin{aligned}
Z_1 &\sim \text{Beta}(1.0, 1.0) \\
Z_2 &\sim \mathcal{N}(1.0, 0.5) \\
X_1 &\sim \mathcal{N}(-2.0, 2.0) \\
X_2 &\sim \text{Beta}(0.0, 0.25) \\
X_3 &\sim t(1.0, 1.0) \\
T &\sim \text{Binomial}(0.5 + 0.4X_1 + 0.3Z_1 + X_1Z_1 + X_2 + 1.5X_3 + 2.5X_3 - 0.5X_1X_3 + Z_2) \\
Y \mid \text{do}(T) &\sim \mathcal{N}(3.0T, 1.0)
\end{aligned} \tag{20}$$

We use a multivariate Gaussian copula to introduce dependencies between the covariates and the causal effect distribution. The Spearman correlation matrix for the copula is

$$R_1 = \begin{pmatrix} 1.0 & 0.8 & 0.8 & 0.8 & 0.8 & 0.8 \\ 0.8 & 1.0 & 0.8 & 0.8 & 0.8 & 0.8 \\ 0.8 & 0.8 & 1.0 & 0.8 & 0.8 & 0.8 \\ 0.8 & 0.8 & 0.8 & 1.0 & 0.8 & 0.8 \\ 0.8 & 0.8 & 0.8 & 0.8 & 1.0 & 0.8 \\ 0.8 & 0.8 & 0.8 & 0.8 & 0.8 & 1.0 \end{pmatrix} \tag{21}$$

**FrugalFlows Sim1** We train a FrugalFlows simulator for this dataset, using the hyperparameters shown in Table 7.

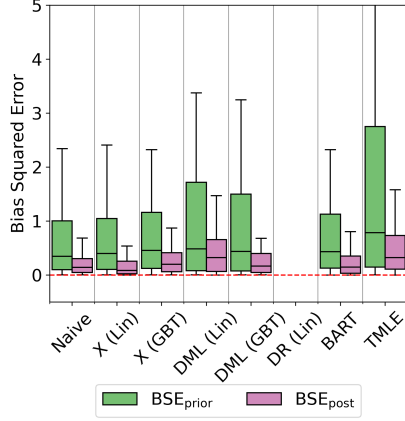
Table 7: FrugalFlows hyperparameters for Frugal Sim1.

Hyperparameter	Value
RQS knots	2
Flow layers	1
Learning rate	0.0054
Network Depth	3
Network Width	9
Causal model (CM)	Location translation
(CM) RQS knots	7
(CM) Flow layers	8
(CM) Network Depth	6
(CM) Network Width	6

**Prior** We specify a single value for the causal effect parameter  $\tau$  and  $\rho$  while generating the datasets from the simulator. The prior is given by

$$\begin{aligned}
\text{Prior}(\tau) &\sim U[0.0, 10.0] \\
\text{Prior}(\rho) &\sim U[-1.0, 1.0]
\end{aligned} \tag{22}$$

**Evaluation** We include the classifier AUC and BSE for the estimators in Figure 25.



	Prior	Posterior
AUC	$0.84 \pm 0.15$	$0.58 \pm 0.01$
<b>Mean BSE</b>		
Diff. of Means	0.748	0.227
X (Lin)	0.857	0.196
X (GBT)	1.027	0.307
DML (Lin)	1.297	0.461
DML (GBT)	1.007	0.308
DR (Lin)	3e7	3e7
BART	0.982	0.262
TMLE	1.779	0.620

Figure 25: Classifier AUC and Mean BSE of causal estimators for DGP: FrugalParam DGP1 and Simulator: FrugalFlows Sim1. (Note the large bias squared error for the estimates of the DR (Lin) estimator).

## E.2 Frugal DGP2

**Frugal DGP2** We use a similar dataset as Frugal DGP1, but vary the correlation matrix and the dependence between the variables as follows

$$\mathbf{R}_2 = \begin{pmatrix} 1.0 & 0.8 & 0.2 & 0.3 & 0.2 & 0.7 \\ 0.8 & 1.0 & 0.1 & 0.4 & 0.9 & 0.3 \\ 0.2 & 0.1 & 1.0 & 0.5 & 0.8 & 0.1 \\ 0.3 & 0.4 & 0.5 & 1.0 & 0.9 & 0.5 \\ 0.2 & 0.9 & 0.8 & 0.9 & 1.0 & 0.6 \\ 0.7 & 0.3 & 0.1 & 0.5 & 0.6 & 1.0 \end{pmatrix} \quad (23)$$

**FrugalFlows Sim2** We simulate data using FrugalFlows with the hyperparameters shown in Table 8.

Table 8: FrugalFlows hyperparameters for Frugal Sim2

Hyperparameter	Value
RQS knots	6
Flow layers	6
Learning rate	0.0027
Network Depth	7
Network Width	9
Causal model (CM)	Location translation
(CM) RQS knots	6
(CM) Flow layers	5
(CM) Network Depth	2
(CM) Network Width	9

We introduce some model misspecification in this experiment, by using a single value for the DGP parameter  $\rho$  to approximate the dependence between all the covariates and the causal effect distribution.

### Prior

$$\begin{aligned} \text{Prior}(\tau) &\sim U[0.0, 10.0] \\ \text{Prior}(\rho) &\sim U[-1.0, 1.0] \end{aligned} \quad (24)$$

**Evaluation** We include the classifier AUC and mean BSE for the estimators in Figure 26, and note that both the  $AUC_{\text{post}}$  and the  $BSE_{\text{post}}$  are lower than the corresponding prior values, indicating that the posterior estimates are informative.

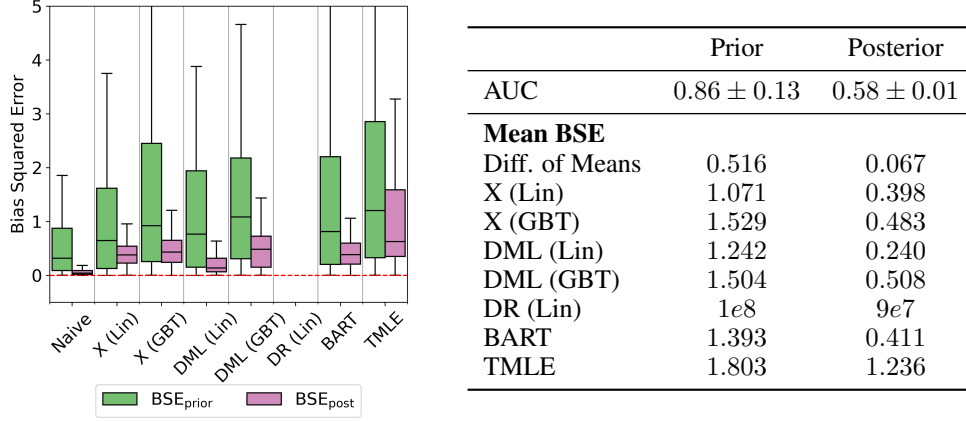


Figure 26: Classifier AUC and Mean BSE of causal estimators for DGP: Frugal DGP2 and Simulator: FrugalFlows Sim2.

### E.3 Frugal DGP3

**Frugal DGP3** In this dataset, we have three covariates  $X_1, X_2, X_3$ , a binary treatment  $T$  and outcome  $Y$  for 5000 samples defined using the following model

$$\begin{aligned}
 X_1 &\sim \mathcal{N}(2.0, 1.0) \\
 X_2 &\sim \text{Gamma}(1.0, 1.0) \\
 X_3 &\sim \mathcal{N}(3.0, 1.0) \\
 T &\sim \text{Binomial}(-0.3X_1 + 0.3X_2 - 0.4X_3 - 0.1X_1X_2) \\
 Y \mid \text{do}(T) &\sim \mathcal{N}(5.0T, 1.5)
 \end{aligned} \tag{25}$$

The dependence between the covariates and the causal effect distribution is modeled using a multi-variate Gaussian copula with the following Spearman correlation matrix

$$\mathbf{R}_3 = \begin{pmatrix} 1.0 & 0.0 & 0.0 & -0.5 \\ 0.0 & 1.0 & 0.0 & -0.3 \\ 0.0 & 0.0 & 1.0 & 0.9 \\ -0.5 & -0.3 & 0.9 & 1.0 \end{pmatrix} \tag{26}$$

**FrugalFlows Sim3** We trained a FrugalFlows model on the source data using the hyperparameters stated in Table 9. We ran two version of the simulator, one without unobserved confounding, by setting the parameter  $\rho = 0.0$ , and another with unobserved confounding by dropping the covariate  $X_2$  from the source data. We call the second setup FrugalFlows Sim3(u) and show the priors for both settings below. The hyperparameters for the dataset with unobserved confounding are also included in Table 9.

**Prior: Sim3**

$$\text{Prior}(\tau) \sim U[0.0, 10.0] \tag{27}$$

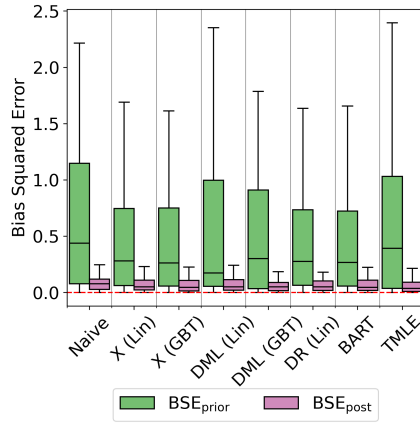
**Prior: Sim3(u)**

$$\begin{aligned}
 \text{Prior}(\tau) &\sim U[0.0, 10.0] \\
 \text{Prior}(\rho) &\sim U[-1.0, 1.0]
 \end{aligned} \tag{28}$$

**Evaluation** We compute the classifier AUC and mean BSE for causal estimators for FrugalFlows Sim3 in Figure 27 and FrugalFlows Sim3(u) in Figure 28. In both cases, the posterior estimates are informative and similar to the source data.

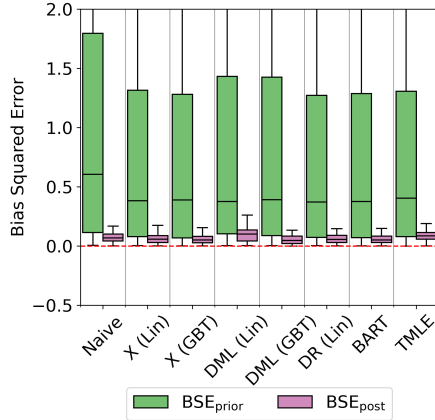
Table 9: FrugalFlows hyperparameters for FrugalFlows Sim3 and FrugalFlows Sim 3(u)

	FrugalFlows Sim3	FrugalFlows Sim3(u)
Hyperparameter	Value	
RQS knots	2	8
Flow layers	1	11
Learning rate	0.0061	0.0215
Network Depth	4	3
Network Width	39	89
Causal model (CM)	Location translation	Location translation
(CM) RQS knots	15	6
(CM) Flow layers	15	4
(CM) Network Depth	53	62
(CM) Network Width	75	62



	Prior	Posterior
AUC	$0.68 \pm 0.04$	$0.53 \pm 0.01$
<b>Mean BSE</b>		
Diff. of Means	0.868	0.097
X (Lin)	0.633	0.069
X (GBT)	0.610	0.064
DML (Lin)	0.601	0.077
DML (GBT)	0.695	0.067
DR (Lin)	0.595	0.067
BART	0.616	0.064
TMLE	0.773	0.062

Figure 27: Classifier AUC and Mean BSE of causal estimators for DGP: Frugal DGP3 and Simulator: FrugalFlows Sim3.



	Prior	Posterior
AUC	$0.68 \pm 0.05$	$0.52 \pm 0.01$
<b>Mean BSE</b>		
Diff. of Means	1.175	0.087
X (Lin)	0.968	0.071
X (GBT)	0.923	0.065
DML (Lin)	1.031	0.108
DML (GBT)	0.972	0.063
DR (Lin)	1.028	0.072
BART	0.927	0.066
TMLE	0.910	0.098

Figure 28: Classifier AUC and Mean BSE of causal estimators for DGP: Frugal DGP3 and Simulator: FrugalFlows Sim3(u).

#### F.4 Frugal DGP4

**FrugalDGP4** This dataset is based on the simulator in the FrugalFlows [de Vassimon Manela et al., 2024] paper (referred to as  $M_1$  in the original paper). We have four covariates  $X_1..X_4$ , a binary treatment  $T$ , and outcome  $Y$ . We describe the full data generating process as shown below.

$$\begin{aligned}
X_1 &\sim \text{Gamma}(\mu = 1, \phi = 1) \\
X_2 &\sim \text{Gamma}(\mu = 1, \phi = 1) \\
X_3 &\sim \text{Gamma}(\mu = 1, \phi = 1) \\
X_4 &\sim \text{Gamma}(\mu = 1, \phi = 1) \\
T &\sim \text{Binomial}(-2 + X_1 + X_2 + X_3 + X_4) \\
Y \mid \text{do}(T) &\sim \mathcal{N}(0.5 + 5T, 1)
\end{aligned} \tag{29}$$

The gaussian dependency matrix  $R_4$  is given by

$$\mathbf{R}_4 = \begin{pmatrix} 1.0 & 0.5 & 0.3 & 0.1 & 0.8 \\ 0.5 & 1.0 & 0.4 & 0.1 & 0.8 \\ 0.3 & 0.4 & 1.0 & 0.1 & 0.8 \\ 0.1 & 0.1 & 0.1 & 1.0 & 0.8 \\ 0.8 & 0.8 & 0.8 & 0.8 & 1.0 \end{pmatrix} \tag{30}$$

**FrugalParam Sim4(u)** For this dataset, we use a simulator that is based on the frugal parameterization method, called FrugalParam Sim4(u). This experiment is a sanity check to verify the informativeness of the selected DGP parameters. We drop the covariate  $X_4$  from the dataset to simulate unobserved confounding, and treat the last column of matrix  $R_4$  as the unobserved confounding bias. The simulator is as described below

$$\begin{aligned}
X_1 &\sim \text{Gamma}(\mu = 1, \phi = 1) \\
X_2 &\sim \text{Gamma}(\mu = 1, \phi = 1) \\
X_3 &\sim \text{Gamma}(\mu = 1, \phi = 1) \\
X_4 &\sim \text{Gamma}(\mu = 1, \phi = 1) \\
T &\sim \text{Binomial}(-2 + X_1 + X_2 + X_3 + X_4) \\
Y \mid \text{do}(T) &\sim \mathcal{N}(0.5 + \tau T, 1)
\end{aligned} \tag{31}$$

**Prior: FrugalParam Sim4(u)** The prior is given by

$$\begin{aligned}
\text{Prior}(\tau) &\sim U[-20.0, 20.0] \\
\text{Prior}(\rho) &\sim U[-1.0, 1.0]
\end{aligned} \tag{32}$$

**Evaluation** The classifier AUC and BSE are displayed in Figure 29.

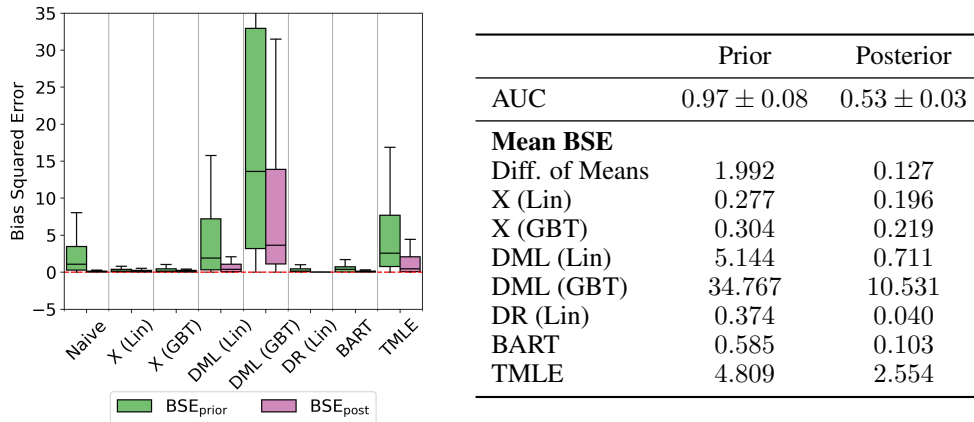


Figure 29: Classifier AUC and Mean BSE of causal estimators for DGP: Frugal DGP4 and Simulator: FrugalParam Sim4(u).

**FrugalFlows Sim4 and FrugalFlows Sim4(u)** For this experiment, we also train FrugalFlows as the simulator using two versions: with and without unobserved confounding. These simulators are described as FrugalFlows Sim4 and FrugalFlows Sim4(u) respectively. As stated earlier, to simulate unobserved confounding, we drop the covariate  $X_4$  from the data. The hyperparameters for both simulators are shown in Table 10.

Table 10: FrugalFlows hyperparameters for FrugalFlows Sim4 and FrugalFlows Sim4(u).

	FrugalFlows Sim4	FrugalFlows Sim4(u)
Hyperparameter	Value	
RQS knots	3	3
Flow layers	1	1
Learning rate	0.0077	0.0597
Network Depth	1	1
Network Width	98	58
Causal model (CM)	Location translation	Location translation
(CM) RQS knots	5	4
(CM) Flow layers	3	2
(CM) Network Depth	78	68
(CM) Network Width	84	69

**Prior: FrugalFlows Sim4** The prior is given by

$$\text{Prior}(\tau) \sim U[-20.0, 20.0] \quad (33)$$

**Prior: FrugalParam Sim4(u)** The prior is given by

$$\begin{aligned} \text{Prior}(\tau) &\sim U[-20.0, 20.0] \\ \text{Prior}(\rho) &\sim U[-1.0, 1.0] \end{aligned} \quad (34)$$

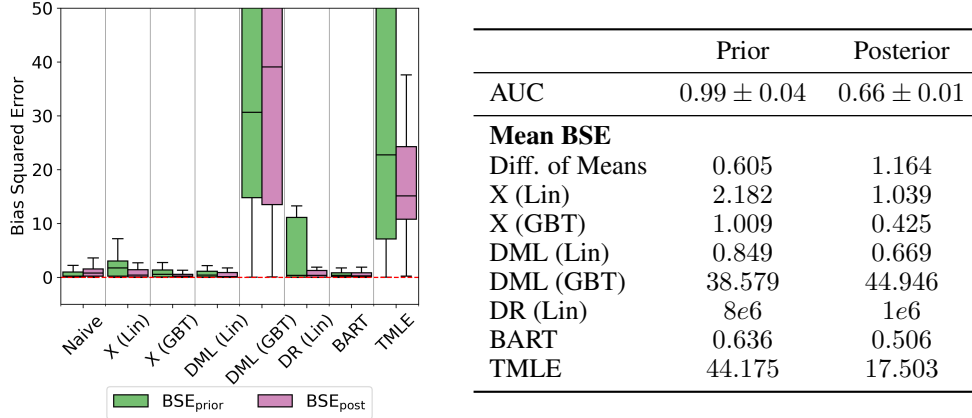
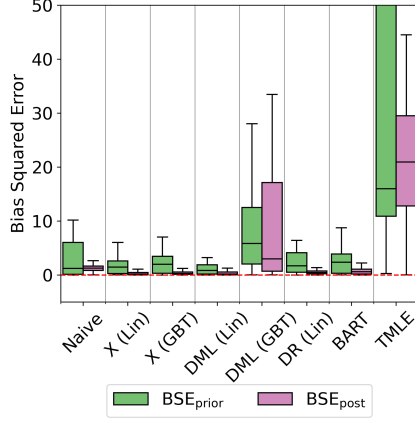


Figure 30: Classifier AUC and Mean BSE of causal estimators for DGP: Frugal DGP4 and Simulator: FrugalFlows Sim4.

**Evaluation** We display the classifier AUC and BSE in Figures 30 and 31 respectively.

## F.5 Frugal DGP5

**Frugal DGP5** We replicate model  $M_3$  in the FrugalFlows [de Vassimon Manela et al., 2024] paper for this experiment. It has 10 covariates, which are combination of discrete and continuous covariates  $X_1 \dots X_{10}$ , a binary treatment  $T$  and outcome  $Y$ . The data generating process is as shown below



	Prior	Posterior
AUC	$0.68 \pm 0.04$	$0.53 \pm 0.01$
<b>Mean BSE</b>		
Diff. of Means	2.961	1.305
X (Lin)	1.971	0.315
X (GBT)	2.187	0.415
DML (Lin)	1.226	0.439
DML (GBT)	16.569	12.744
DR (Lin)	1e7	0.628
BART	2.447	0.709
TMLE	48.569	21.788

Figure 31: Classifier AUC and Mean BSE of causal estimators for DGP: Frugal DGP4 and Simulator: FrugalFlows Sim4(u).

$$\begin{aligned}
X_1 &\sim \text{Gamma}(\mu = 1.3, \phi = 1) \\
X_2 &\sim \text{Gamma}(\mu = 1.3, \phi = 1) \\
X_3 &\sim \text{Gamma}(\mu = 1.3, \phi = 1) \\
X_4 &\sim \text{Gamma}(\mu = 1.3, \phi = 1) \\
X_5 &\sim \text{Gamma}(\mu = 1.3, \phi = 1) \\
X_6 &\sim \text{Bernoulli}(p = 0.5) \\
X_7 &\sim \text{Bernoulli}(p = 0.5) \\
X_8 &\sim \text{Bernoulli}(p = 0.5) \\
X_9 &\sim \text{Bernoulli}(p = 0.5) \\
X_{10} &\sim \text{Bernoulli}(p = 0.5) \\
T &\sim \text{Bernoulli}(-0.3 + 0.1X_1 + 0.2X_2 + 0.5X_3 - 0.2X_4 + 1X_5 + 0.3X_6 - 0.4X_7 + 0.7X_8 - 0.1X_9 + 0.9X_{10}) \\
Y \mid \text{do}(T) &\sim \mathcal{N}(2.5 - 5T, 1)
\end{aligned} \tag{35}$$

The gaussian dependency matrix  $R_5$  is given by

$$R_5 = \begin{pmatrix}
1.0 & 0.3 & 0.4 & 0.5 & 0.1 & -0.2 & -0.7 & 0.5 & -0.4 & 0.5 \\
0.3 & 1.0 & -0.3 & 0.6 & -0.3 & 0.4 & -0.4 & 0.6 & 0.3 & 0.2 \\
0.4 & -0.3 & 1.0 & -0.5 & 0.2 & -0.1 & -0.1 & 0.0 & -0.4 & -0.4 \\
0.5 & 0.6 & -0.5 & 1.0 & -0.2 & -0.2 & -0.5 & 0.5 & 0.3 & 0.4 \\
0.1 & -0.3 & 0.2 & -0.2 & 1.0 & -0.1 & -0.1 & -0.5 & -0.6 & -0.2 \\
-0.2 & 0.4 & -0.1 & -0.2 & -0.2 & 1.0 & 0.0 & 0.4 & 0.2 & 0.5 \\
-0.7 & -0.4 & -0.1 & -0.5 & -0.1 & 0.0 & 1.0 & -0.5 & 0.4 & -0.4 \\
0.5 & 0.6 & 0.0 & 0.5 & -0.5 & 0.5 & -0.5 & 1.0 & 0.4 & 0.4 \\
-0.4 & 0.3 & -0.4 & 0.3 & -0.6 & 0.2 & 0.4 & 0.4 & 1.0 & 0.4 \\
0.5 & 0.2 & -0.4 & 0.4 & -0.2 & 0.5 & -0.4 & 0.4 & 0.4 & 1.0
\end{pmatrix} \tag{36}$$

**FrugalFlows Sim5 and FrugalFlows Sim5(u)** We train two simulators FrugalFlows Sim5 and FrugalFlows Sim5(u). To simulate unobserved confounding, we drop the covariates  $X_3$  and  $X_7$ . The hyperparameters for both simulators are displayed in Table 11.

**Prior: FrugalFlows Sim5** The prior is given by

$$\text{Prior}(\tau) \sim U[-20.0, 20.0] \tag{37}$$

**Prior: FrugalParam Sim5(u)** The prior is given by

$$\begin{aligned}
\text{Prior}(\tau) &\sim U[-20.0, 20.0] \\
\text{Prior}(\rho) &\sim U[-1.0, 1.0]
\end{aligned} \tag{38}$$



Table 11: FrugalFlows hyperparameters for FrugalFlows Sim5 and FrugalFlows Sim5(u).

	FrugalFlows Sim5	FrugalFlows Sim5(u)
Hyperparameter	Value	
RQS knots	1	1
Flow layers	1	4
Learning rate	0.0081	0.0043
Network Depth	50	77
Network Width	22	39
Causal model (CM)	Location translation	Location translation
(CM) RQS knots	5	9
(CM) Flow layers	5	3
(CM) Network Depth	31	56
(CM) Network Width	1	36

**Evaluation** The classifier AUC and BSE are displayed in Figures 32 and 33.

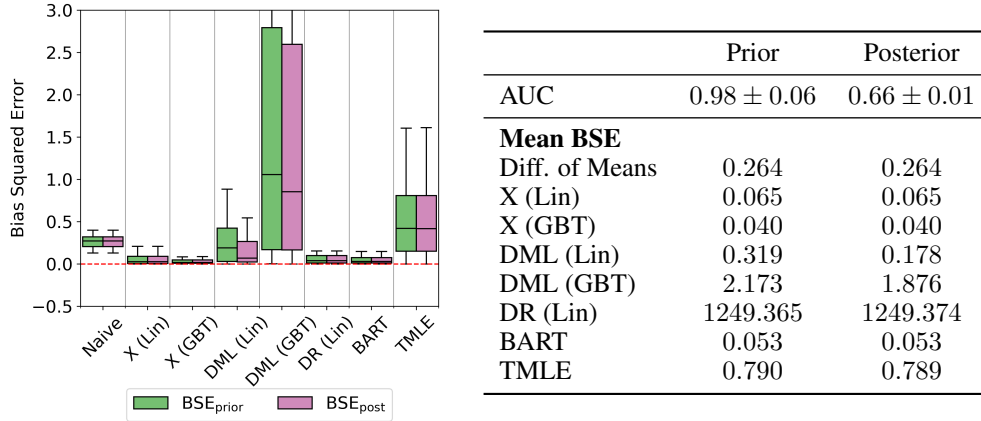


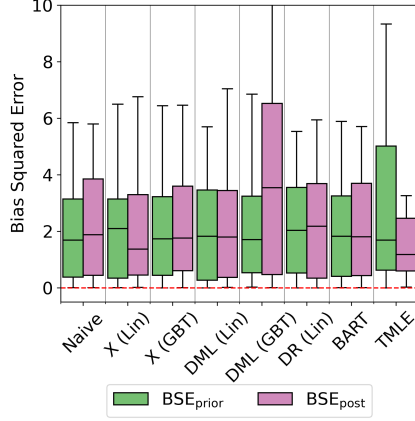
Figure 32: Classifier AUC and Mean BSE of causal estimators for DGP: Frugal DGP5 and Simulator: FrugalFlows Sim5.

#### Key takeaway

As long as the simulator is able to approximate the source data distribution, computing the posterior is informative, i.e. we may be able to eliminate values of the DGP parameters that are incompatible with the source data distribution. We verified this is true for non-parametric DGPs and flexible, neural-network based simulators (FrugalFlows).

## G Evaluating SBICE on real-world, observational datasets

Apart from synthetic datasets, we also evaluated SBICE on real-world, observational datasets. We used datasets that are commonly used as benchmarks in the causal inference literature. We chose datasets that had an experimental arm so that we had a ground-truth estimate of the ATE for the source dataset, as it allowed us to compute the bias squared error (BSE) for each of them. We focused on the DGP parameter  $\theta = \{\tau\}$  for these datasets, by making an assumption of no unobserved confounding. For the real-world datasets, we found that the posterior datasets and the causal estimators on the posterior datasets were similar to that of the prior. We attribute these observations to two key reasons: (1) the small sample size of the real-world datasets impeded the simulator from learning the exact distributions of the source data; and (2) many of the causal estimators were invariant to the change in the set of DGP parameters.



	Prior	Posterior
AUC	$0.97 \pm 0.07$	$0.71 \pm 0.14$
<b>Mean BSE</b>		
Diff. of Means	1.955	2.249
X (Lin)	2.157	2.034
X (GBT)	2.033	2.224
DML (Lin)	2.179	2.195
DML (GBT)	2.880	4.193
DR (Lin)	4e5	5e5
BART	2.013	2.149
TMLE	3.171	2.114

Figure 33: Classifier AUC and Mean BSE of causal estimators for DGP: Frugal DGP5 and Simulator: FrugalFlows Sim5(u).

### G.1 Lalonde (Exp)

This dataset has 8 covariates (a combination of discrete and continuous values). It is based on the randomized controlled trial that examines the impact of an employment program on the income levels of participants. There is no unobserved confounding, as this is an RCT.

**Simulator** We trained the FrugalFlows simulator for this dataset, referred to as the FrugalFlows Real1. The hyperparameters used are shown in Table 12.

Table 12: FrugalFlows hyperparameters for FrugalFlows Real1

Hyperparameter	Value
RQS knots	20
Flow layers	14
Learning rate	0.001
Network Depth	22
Network Width	11
Causal model (CM)	Location translation
(CM) RQS knots	3
(CM) Flow layers	13
(CM) Network Depth	25
(CM) Network Width	28

**Prior** We set the prior as follows

$$\text{Prior}(\tau) = U[-20, 20] \quad (39)$$

**Evaluation** Since this is an RCT, the difference of means is the ground-truth ATE  $\tau^*$ . We compute the classifier AUC and BSE for a set of causal estimators and include the results in Figure 34. We find that both the posterior and the prior exhibit similar classifier AUC and bias squared error and are close to the source data despite the high classifier AUC score.

### G.2 Lalonde (Obs)

An observational counterpart to the RCT in Section G.1 is the Population Survey of Income Dynamics (PSID) control sample. This dataset contains the treated units from the RCT and the control samples from the observational dataset. We use the same set of covariates, and use the ground-truth ATE as the value obtained in the RCT.

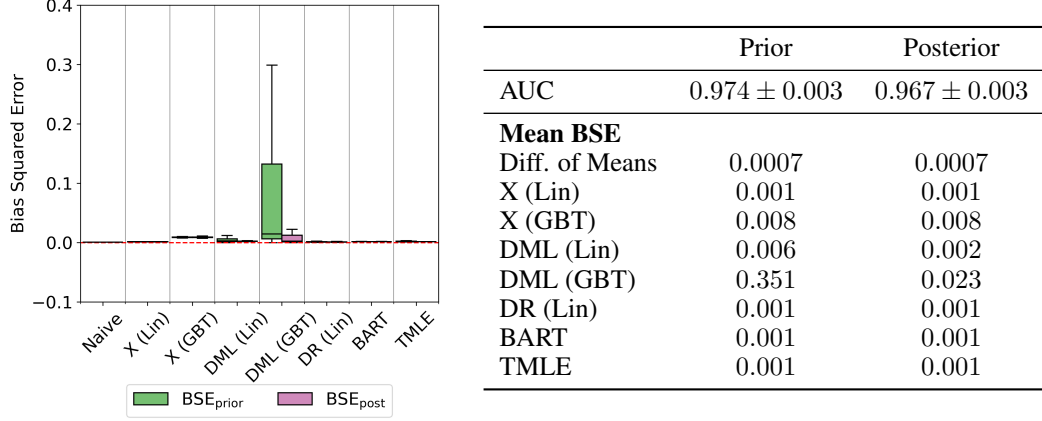


Figure 34: Classifier AUC and Mean BSE of causal estimators for DGP: Lalonde (Exp) and Simulator: FrugalFlows Real1.

**Simulator** We trained FrugalFlows simulator for this dataset, referred to as FrugalFlows Real2. The hyperparameters used are shown in Table 13.

Table 13: FrugalFlows hyperparameters for FrugalFlows Real2

Hyperparameter	Value
RQS knots	1
Flow layers	8
Learning rate	0.0038
Network Depth	2
Network Width	6
Causal model (CM)	Location translation
(CM) RQS knots	9
(CM) Flow layers	4
(CM) Network Depth	3
(CM) Network Width	6

**Prior** We set the prior as follows

$$\text{Prior}(\tau) = U[-20, 20] \quad (40)$$

**Evaluation** Similar to the RCT, we found that both the posterior and the prior exhibit similar performance. We include the bias squared error plot in Figure 35.

### G.3 Project STAR

For the third real-world dataset, we used the Project STAR (Student-Teacher Achievement Ratio) dataset, which was an experiment that was designed to study the effect of class size on student performance. We followed the methods described in the Credence [Parikh et al., 2022] to extract this dataset, and used an unbiased estimate of the difference of means from the experimental arm as the ground-truth ATE.

**Simulator** We trained FrugalFlows on this dataset, referred to as FrugalFlows Real3. The hyperparameters are shown in Table 14.

**Prior** We set the prior as follows

$$\text{Prior}(\tau) = U[-20, 20] \quad (41)$$

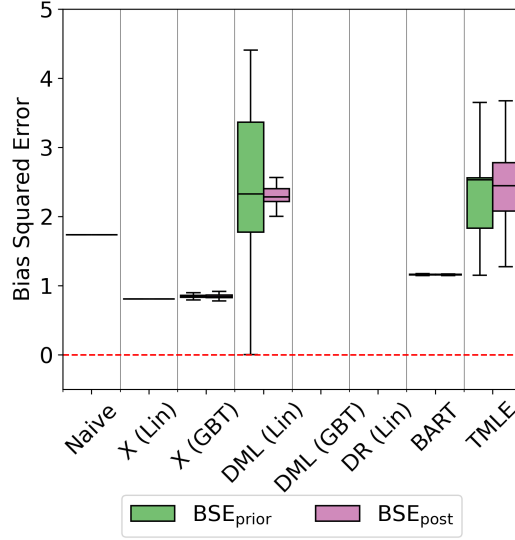


Figure 35: Bias squared error for causal estimators for the Lalonde (obs) dataset

Table 14: FrugalFlows hyperparameters for FrugalFlows Real3

Hyperparameter	Value
RQS knots	20
Flow layers	8
Learning rate	0.0002
Network Depth	4
Network Width	15
Causal model (CM)	Location translation
(CM) RQS knots	4
(CM) Flow layers	13
(CM) Network Depth	33
(CM) Network Width	10

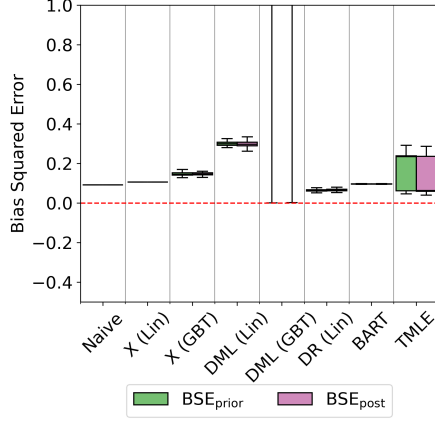
**Evaluation** Similar to the RCT, we found that both the posterior and the prior exhibit similar performance. We include the results in Figure 36. We also include the results of experiments where we imposed a prior over  $\text{Prior}(\rho) \sim U[-1, 1]$ . We found that the simulator was unable to model the confounding bias present in the real data (if any), as the posterior estimates were similar to the prior. The results are included in Figure 37.

#### Key takeaway

For real-world observational datasets with small samples, we found that the existing simulators were unable to accurately model the source data distributions (indicated by the high classifier AUCs). In such cases, the posterior and prior exhibited similar properties (classifier AUC and BSE).

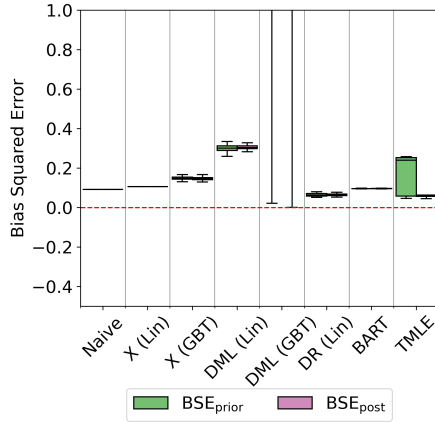
## H Empirical experiments comparing generative methods across fixed point estimates of DGP parameters

In this section, we outline the results of our experiments comparing generative methods for the same source dataset. We perform two types of comparisons: (1) across generative methods without setting any values for DGP parameters, and (2) setting constraints on the ATE for each generative method. This section expands on the results presented in Section 2. We perform this analysis across a variety



	Prior	Posterior
AUC	$0.935 \pm 0.004$	$0.932 \pm 0.003$
<b>Mean BSE</b>		
Diff. of Means	0.092	0.092
X (Lin)	0.105	0.105
X (GBT)	0.146	0.146
DML (Lin)	0.290	0.284
DML (GBT)	10.670	8.773
DR (Lin)	0.063	0.065
BART	0.095	0.095
TMLE	0.163	0.140

Figure 36: Classifier AUC and Mean BSE of causal estimators for DGP: Project STAR and Simulator: FrugalFlows Real3.



	Prior	Posterior
AUC	$0.939 \pm 0.003$	$0.929 \pm 0.001$
<b>Mean BSE</b>		
Diff. of Means	0.092	0.092
X (Lin)	0.105	0.105
X (GBT)	0.147	0.146
DML (Lin)	0.310	0.302
DML (GBT)	15.669	9.360
DR (Lin)	$1e5$	0.064
BART	0.095	0.095
TMLE	0.174	0.106

Figure 37: Classifier AUC and Mean BSE of causal estimators for DGP: Project STAR and Simulator: FrugalFlows Real3.

of source datasets, generated using simple, synthetic data-generating processes to real-world datasets. To compare the differences between generative methods, we compute the AUC of a classifier trained to distinguish between the source and generated datasets, and report the cross-validated AUC for every experiment. In addition, we also compute the bias (estimated ATE — true ATE) for a set of causal estimators.

We use four different generative methods: Credence, modified-Credence, Realcause and FrugalFlows. As it is computationally intensive to train generative methods such as Credence and modified-Credence for every constraint imposed for a dataset, we compare across constraints on the DGP parameters for a few datasets. We observe that for small sample settings or when the datasets have a large number of covariates, the differences between generative methods are more pronounced than others. We also note that some methods have larger differences between constraints when compared to others. We highlight some of these observations for each dataset.

## H.1 Synthetic datasets

### H.1.1 LinearParam DGP11

We designed a dataset using 3 covariates  $X_1 \dots X_3$ , a binary treatment  $T$  and outcome  $Y$  with the data-generating process as shown below.

$$\begin{aligned}
X_1 &\sim \mathcal{N}(0, 1) \\
X_2 &\sim \text{Exponential}(\lambda = 0.5) \\
X_3 &\sim \mathcal{N}(1, 1) \\
T &\sim \text{Binomial} \left( \text{Expit} \left( \frac{X_1 + X_2 + X_3}{3} + \mathcal{N}(0, 0.1) \right) \right) \\
Y &\sim \mathcal{N}(\mu = X_1 + X_2 + X_3 + 3T, 0.1)
\end{aligned} \tag{42}$$

We generated datasets with 9000 samples, and eliminated those rows which exhibited positivity/overlap violations, leaving us with a dataset around 8000 samples. For this dataset, we trained all the generative methods under three settings

1. Learned ATE: We did not set any constraints to the generative method, and learned the distributions from the source data.
2. True ATE: We set the constraint that the true ATE  $\tau = 3.0$  (obtained from the data generating process).
3. Incorrect ATE: We set the constraint that the ATE  $\tau = 10.0$  (a large, positive value compared to the ground-truth).

To evaluate the differences across generative methods as well as the settings, we compared the generated datasets to the source dataset and computed the mean classifier AUC score across 50 generated datasets. The classifier AUC score for datasets generated using generative method  $\mathcal{G}$  with constraint  $\tau$  is given by

$$\text{AUC}_{\mathcal{G};\tau} = \text{AUC}(R(D_{\text{source}}, \hat{D}_{\mathcal{G};\tau}))$$

where  $R$  is a binary classifier trained to distinguish between the generated and source datasets. An AUC close to 0.5 indicates that the generated datasets are similar to that of the source data. The AUC score is displayed in Table 15.

Table 15: Classifier AUC for LinearParam DGP11 across generative methods and three settings of the ATE parameter.

	Credence	mod-Credence	Realcause	FrugalFlows
Learned ATE	$0.959 \pm 0.001$	$0.691 \pm 0.001$	$0.922 \pm 0.002$	$0.491 \pm 0.006$
True ATE	$0.999 \pm 0.0$	$1.0 \pm 0.0$	$0.921 \pm 0.002$	$0.491 \pm 0.006$
Incorrect ATE	$0.999 \pm 0.0$	$0.999 \pm 0.0$	$0.976 \pm 0.001$	$0.881 \pm 0.002$

We also looked at the underlying marginal distributions of the generated datasets across generative methods to study the differences between them. For a single generated dataset, we plot the marginal distribution of the outcome  $Y$  across all three settings in Figure 38. While most methods learn the same marginal distribution of the outcome for the flexible setting, we find that setting constraints on Credence and modified-Credence have the largest impact on the marginal distribution of the generated datasets. These differences arise from how the constraints are imposed on the generative method. Realcause and FrugalFlows scales the learned distribution post-hoc to adjust for the difference in outcome, but Credence and modified-Credence add the constraint to the loss function directly.

In addition, we also compared the ATE of the generated datasets across generative methods and constraints. We display them in Figure 39. This figure highlights that while most of the generative methods satisfy the user-defined constraints on the DGP parameters, they learned different distributions of the data when there are no constraints. Specifically, we note that Credence and Realcause show differences in the learned ATE values even for a simple, linear dataset.

Finally, we estimated the ATE for the generated datasets using a set of causal estimators. We plot the bias of the estimator across 50 generated datasets in Figure 40 for all the settings described above. We found that for this dataset, the bias of all causal estimators were similar to each other in most cases, with the exception of the Credence in the learned ATE setting (see Figure 40a).

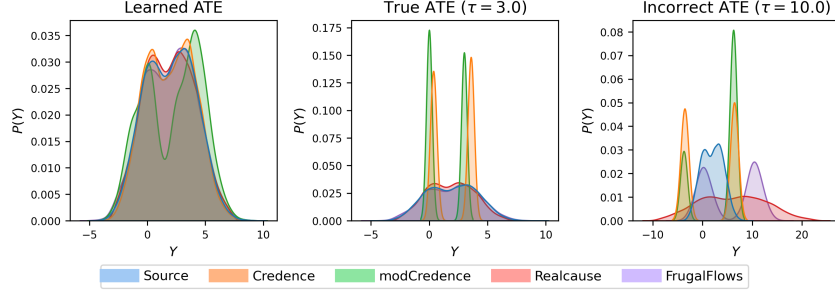


Figure 38: Marginal distribution of outcome  $Y$  for LinearParam DGP11.

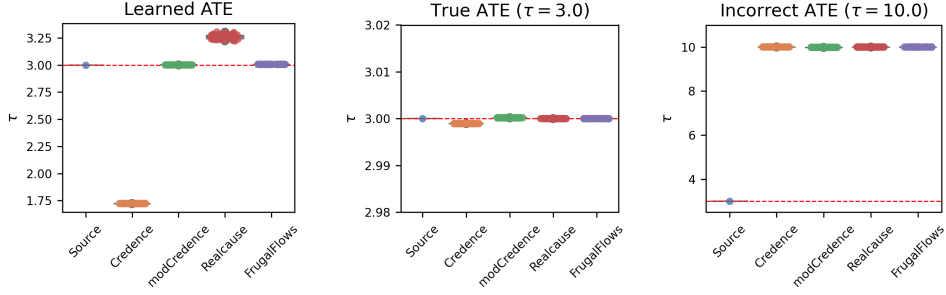


Figure 39: ATEs for the generated datasets across generative methods for the three different settings of the constraints.

**Key Takeaway** We find that even for a simplistic, synthetic dataset with linear relationships and smaller number of covariates, the differences between generative methods is large, especially with the flexible setting (no constraints imposed on the dataset).

### H.1.2 Param DGP12

We compare generative methods for datasets with a larger number of covariates, and potentially non-linear relationships between variables. We use a set of datasets originally defined by the authors of the X-Learner metalearner [Künzel et al., 2019]. This dataset is derived from the simulation SI 6 in the original paper. For simplicity, we show the data-generating process here

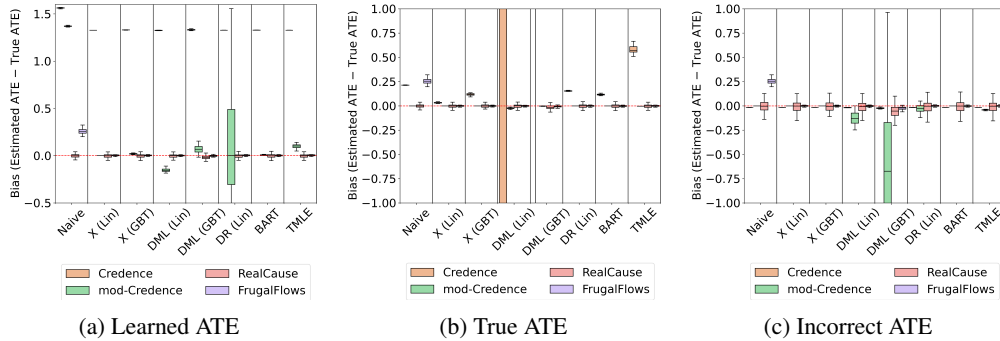


Figure 40: Boxplots of the bias (estimated ATE – true ATE) for a set of causal estimators for all generative methods across three different settings for the Synthetic DGP1 dataset.

$$\begin{aligned}
X &\sim \text{Uniform}([0, 1]^{N \times 20}) \\
e(X) &= \frac{1}{4}(1 + \text{Beta}(X_1, 2, 4)) \\
\mu_0(X) &= 2X_1 - 1 \\
\mu_1(X) &= \mu_0(X)
\end{aligned} \tag{43}$$

In the above data generating process, we have 20 covariates  $X_1 \dots X_{20}$  which are all derived from a uniform distribution.  $e(X)$  denotes the propensity score and the relationship between the binary treatment and covariates, and the notation  $\text{Beta}(X_1, 2, 4)$  denotes a Beta distribution with parameters 2 and 4. The outcome for the control group is denoted by  $\mu_0(X)$ , which is based on the covariate  $X_1$ . The true ATE is 0.0 as the treated units are similar to that of the control units. We generate  $N = 2000$  samples

For this dataset, we only learn the generative model under the flexible setting (without imposing any constraints on the DGP parameters). We use the AUC score to measure the similarity of the generated datasets to the source data, and show the results in Table 41. We also include the bias of a set of causal estimators for the generated datasets in Figure 42. We note that apart from Credence, all other generated methods show similarity in the performance across all estimators.

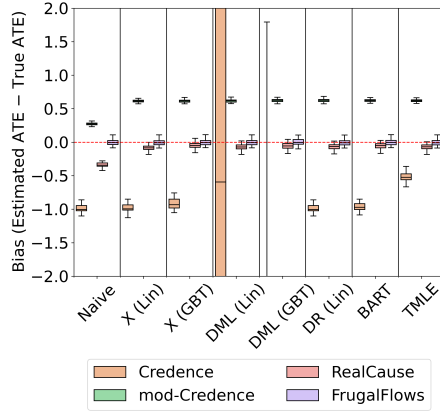


Figure 41: Mean and Standard deviation of Classifier AUC scores for each method under the Learned ATE setting.

Gen. method	AUC
Credence	$1.0 \pm 0.0$
Modified Credence	$1.0 \pm 0.0$
Realcause	$1.0 \pm 0.0$
Frugal Flows	$0.592 \pm 0.012$

Figure 42: The Bias and Classifier AUC for learned ATE setting across all methods: Param DGP12

### H.1.3 Param DGP13

We use the simulation SI 2 in the X-Learner [Künzel et al., 2019] paper. This dataset contains 20 covariates, and represents a dataset without any confounding relationship between the treatment and the covariates. The data generating process is given below.

$$\begin{aligned}
X &\sim \mathcal{N}(0, \Sigma) \\
e(X) &= 0.5 \\
\mu_1(X) &= X^T \beta_1, \text{ with } \beta_1 \sim \text{Unif}([1, 30]^{20}) \\
\mu_0(X) &= X^T \beta_0, \text{ with } \beta_0 \sim \text{Unif}([1, 30]^{20})
\end{aligned} \tag{44}$$

We generate datasets under the flexible setting for all generative methods (without constraints on DGP parameters). The classifier AUC scores and bias of causal estimators is depicted in Figure 44.

### H.1.4 Param DGP14

We repeat this experiment for simulation SI 4 in the X-Learner [Künzel et al., 2019] paper. This dataset contains 5 covariates with the data generating process described below. We generate 2000 samples.



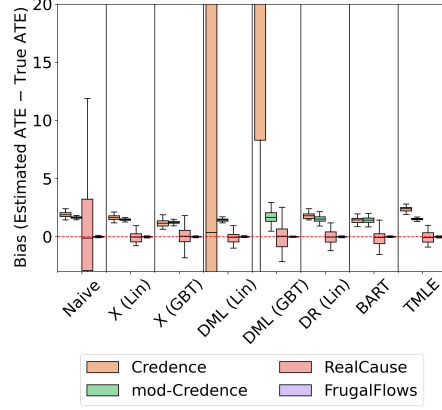


Figure 43: Mean and Standard deviation of Classifier AUC scores for each method under the Learned ATE setting.

Gen. method	AUC
Credence	$1.0 \pm 0.0$
Modified Credence	$1.0 \pm 0.0$
Realcause	$1.0 \pm 0.0$
Frugal Flows	$0.978 \pm 0.001$

Figure 44: The bias and classifier AUC for learned ATE setting across all methods: Param DGP13

$$\begin{aligned}
 X &\sim \text{Uniform}([0, 1]^{N \times 5}) \\
 e(X) &= 0.5 \\
 \mu_0(X) &= X^T \beta \text{ with } \beta \sim \text{Unif}([1, 30]^5) \\
 \mu_1(X) &= \mu_0(X)
 \end{aligned} \tag{45}$$

The bias of the causal estimators and the classifier AUC scores are depicted in Figure 46.

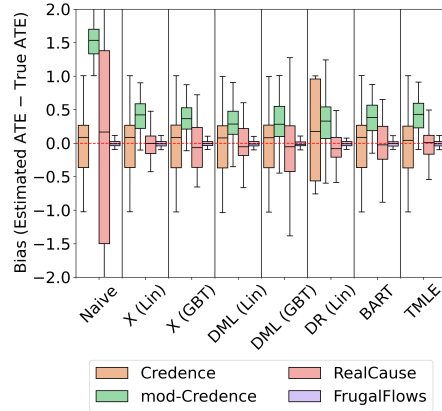


Figure 45: Mean and Standard deviation of Classifier AUC scores for each method under the Learned ATE setting.

Gen. method	AUC
Credence	$1.0 \pm 0.0$
Modified Credence	$1.0 \pm 0.0$
Realcause	$1.0 \pm 0.0$
Frugal Flows	$0.848 \pm 0.006$

Figure 46: The bias and classifier AUC for learned ATE setting across all methods: Param DGP14

### H.1.5 Param DGP15

For simulation SI 5, we generate 2000 samples. This data-generating process describes a piecewise linear model.

$$\begin{aligned}
X &\sim \text{Uniform}([0, 1]^{N \times 20}) \\
e(X) &= 0.5 \\
\mu_0(X) &= \begin{cases} X^T \beta_l & \text{if } X_{20} < -0.4 \\ X^T \beta_m & \text{if } -0.4 \leq X_{20} \leq 0.4 \\ X^T \beta_u & \text{if } 0.4 < X_{20} \end{cases} \\
\mu_1(X) &= \mu_0(X)
\end{aligned} \tag{46}$$

The bias of the causal estimators and the classifier AUC scores are depicted in Figure 48.

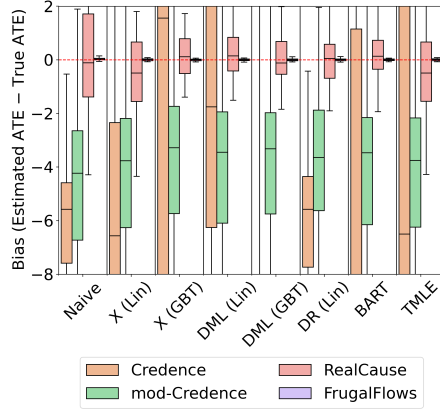


Figure 47: Mean and Standard deviation of Classifier AUC scores for each method under the Learned ATE setting.

Gen. method	AUC
Credence	$1.0 \pm 0.0$
Modified Credence	$1.0 \pm 0.0$
Realcause	$1.0 \pm 0.0$
Frugal Flows	$0.576 \pm 0.009$

Figure 48: The bias and classifier AUC for learned ATE setting across all methods: Param DGP15

## H.2 Real-world observational datasets

We also compare generative methods across real-world observational datasets commonly used as benchmarks in the causal inference literature. This dataset is the Lalonde dataset, previously described in Appendix G. We use both arms - experimental and observational arms. For these datasets, we test three settings for each generative method: (1) Learned ATE (no constraints); (2) True ATE and (3) Incorrect ATE.

### H.2.1 Lalonde (Exp)

We depict the classifier AUC for this dataset in Table 16. We note that across all generative methods, the AUC is high and we attribute this to the small sample sizes of the dataset leading to high error in the output of the generative methods.

Table 16: Classifier AUC for Lalonde (Exp) across generative methods and three settings of the ATE parameter.

	Credence	mod-Credence	Realcause	FrugalFlows
Learned ATE	$0.997 \pm 0.001$	$0.996 \pm 0.0005$	$1.0 \pm 0.0$	$0.959 \pm 0.008$
True ATE	$1.0 \pm 0.0$	$0.997 \pm 0.003$	$1.0 \pm 0.0$	$0.987 \pm 0.004$
Incorrect ATE	$0.999 \pm 0.0$	$0.999 \pm 0.000$	$1.0 \pm 0.0$	$0.995 \pm 0.003$

We plot the marginal distribution of the outcome across settings and generative methods in Figure 49, and note that differences across all methods and settings. We also plot the ATEs of the generated datasets in Figure 50.

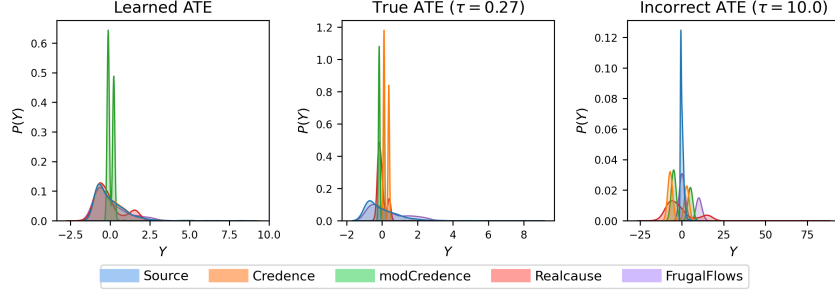


Figure 49: Marginal distribution of outcome  $Y$  for the Lalonde (Exp) datasets.

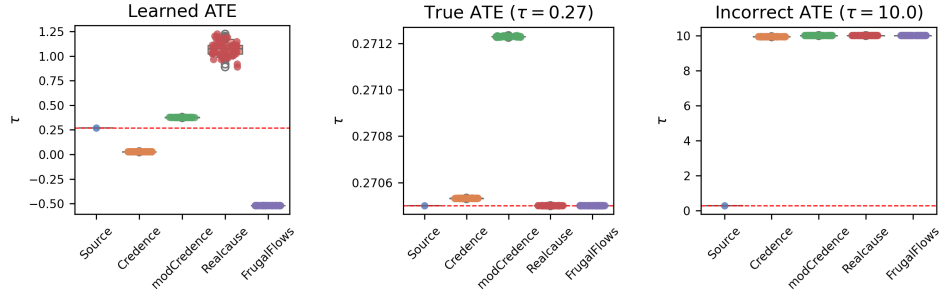


Figure 50: ATEs for the generated datasets across generative methods for the three different settings of the constraints.

The bias of the causal estimators for the Lalonde (Exp) datasets are depicted in Figure 51. We note a high variance in the bias of the estimators for all three settings of the constraints, with no particular pattern to the differences in estimators for a generative method or setting.

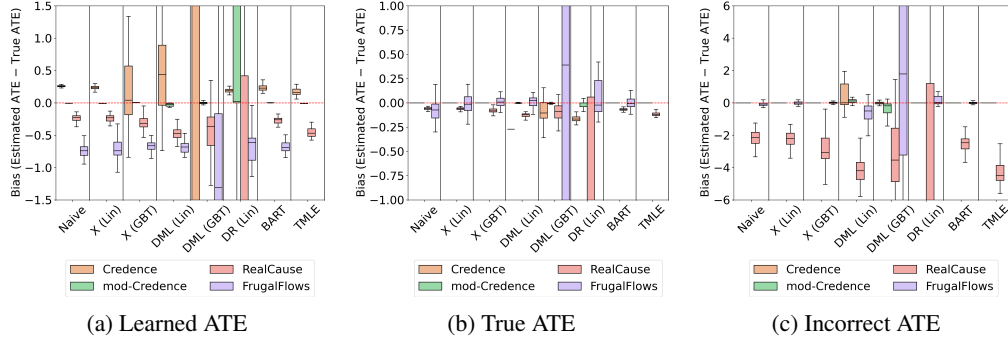


Figure 51: Boxplots of the bias (estimated ATE — true ATE) for a set of causal estimators for all generative methods across three different settings for the Lalonde (Experimental) dataset.

## H.2.2 Lalonde (Obs)

For the observational study, we included the classifier AUC and bias of the datasets across generative methods and settings in Section 2. Here, we supplement these results by including the marginal distribution of the outcome (Figure 52) as well as the ATEs for the generated datasets (Figure 53).

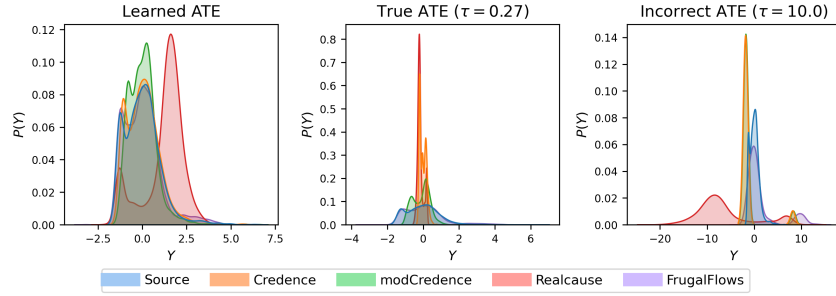


Figure 52: Marginal distribution of outcome  $Y$  for the Lalonde (Obs) datasets.

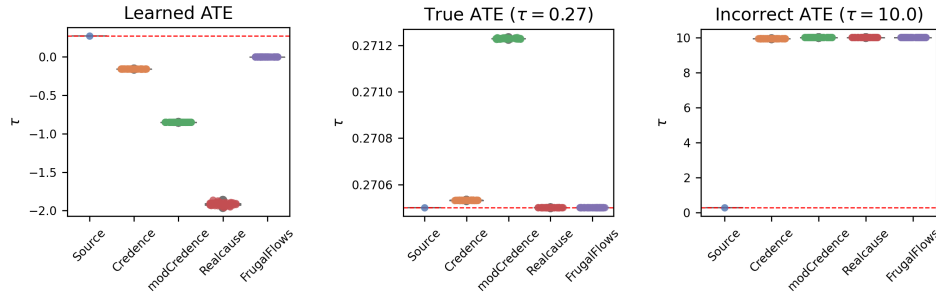


Figure 53: ATEs for the generated datasets across generative methods for the three different settings of the constraints.

### Key takeaway

Across both synthetic and real-world datasets, we observe that different generative methods produce notably different synthetic datasets—even when configured with the same DGP parameter constraints. This divergence persists across sample sizes and highlights the role of inductive biases in shaping the generated counterfactual outcomes. These findings support our theoretical proposition that fixed point estimates of DGP parameters may be incompatible with the source data. Moreover, inconsistencies in the generated datasets lead to variability in causal estimator outputs, complicating sensitivity analyses and making estimator selection less reliable. These challenges motivate the need for a posterior-based approach like SBICE, which explicitly accounts for uncertainty in DGP parameters and improves alignment between generated and source data distributions.